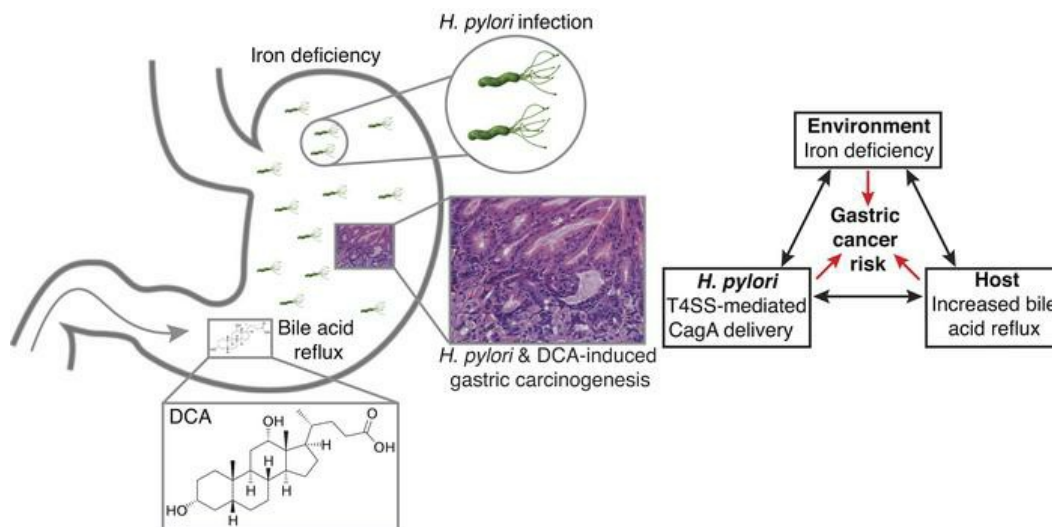# Iron deficiency linked to altered bile acid metabolism promotes *Helicobacter pylori*-induced inflammation-driven gastric carcinogenesis

Jennifer M. Noto, … , Joseph P. Zackular, Richard M. Peek, Jr.

Research   In-Press Preview   Gastroenterology   Infectious disease

Graphical abstract

Iron deficiency linked to altered bile acid metabolism promotes *Helicobacter pylori*-induced inflammation-driven gastric carcinogenesis

Jennifer M. Noto[1], M. Blanca Piazuelo[1], Shailja C. Shah[1*], Judith Romero-Gallo[1], Jessica L. Hart[2], Chao Di[2,3], James D. Carmichael[4*], Alberto G. Delgado[1], Alese E. Halvorson[5], Robert A. Greevy[5], Lydia E. Wroblewski[1], Ayushi Sharma[6], Annabelle B. Newton[7], Margaret M. Allaman[1], Keith T. Wilson[1,8,9], M. Kay Washington[9], M. Wade Calcutt[4], Kevin L. Schey[4], Bethany P. Cummings[10], Charles R. Flynn[11], Joseph P. Zackular[2,12], Richard M. Peek, Jr.[1,9]

[1]Division of Gastroenterology, Department of Medicine, Vanderbilt University Medical Center, Nashville, TN, USA; [2]Division of Protective Immunity, Children's Hospital of Philadelphia, Philadelphia, PA, USA; [3]Department of Biomedical and Health Informatics, Children's Hospital of Philadelphia, Philadelphia, PA, USA; [4]Department of Biochemistry, Mass Spectrometry Research Center Laboratory, Vanderbilt University, Nashville, TN, USA; [5]Department of Biostatistics, Vanderbilt University Medical Center, Nashville, TN, USA; [6]Creighton University School of Medicine, Omaha, NE, USA; [7]Davidson College, Davidson, NC, USA; [8]Department of Veterans Affairs, Tennessee Valley Healthcare System, Nashville, TN, USA, [9]Department of Pathology, Microbiology, and Immunology, Vanderbilt University Medical Center, Nashville, TN, USA; [10]Department of Surgery, University of California, Davis, Davis, CA, USA; [11]Department of Surgery, Vanderbilt University Medical Center, Nashville, TN, USA; [12]Department of Pathology and Laboratory Medicine, University of Pennsylvania, Philadelphia, PA, USA

New affiliations:

[*]Shailja C. Shah: Section of Gastroenterology, Veterans Affairs San Diego Healthcare System, San Diego, CA, USA; The Moores Cancer Center and Division of Gastroenterology, University of California San Diego, La Jolla, CA, USA

[*]James D. Carmichael: Restek Corporation, Bellefonte, PA, USA

Correspondence:

Richard M. Peek, Jr.

Address: Vanderbilt University Medical Center, Department of Medicine, Division of Gastroenterology

2215 Garland Avenue, 1030C Medical Research Building IV, Nashville, TN 37232, USA

Phone: 1-615-322-5200

Email address: richard.peek@vumc.org

ABSTRACT

Gastric carcinogenesis is mediated by complex interactions among *Helicobacter pylori*, host, and environmental factors. We now demonstrate that *H. pylori* augments gastric injury in INS-GAS mice under iron deficient conditions. Mechanistically, these phenotypes were not driven by alterations in the gastric microbiota; however, discovery-based and targeted metabolomics revealed that bile acids were significantly altered in *H. pylori*-infected mice with iron deficiency, with significant upregulation of deoxycholic acid (DCA), a carcinogenic bile acid. Severity of gastric injury was further augmented when *H. pylori*-infected mice were treated with DCA, and, in vitro, DCA increased translocation of the *H. pylori* oncoprotein CagA into host cells. Conversely, bile acid sequestration attenuated *H. pylori*-induced injury under conditions of iron deficiency. To translate these findings into human populations, the association between bile acid-sequestrant use and gastric cancer risk was evaluated in a large human cohort. Among 416,885 individuals, a significant dose-dependent reduction in risk was associated with cumulative bile acid-sequestrant use. Further, expression of the bile acid receptor TGR5 paralleled the severity of carcinogenic lesions in humans. These data demonstrate that increased *H. pylori*-induced injury within the context of iron deficiency is tightly linked to altered bile acid metabolism, which may promote gastric carcinogenesis.

INTRODUCTION

Gastric adenocarcinoma is the third leading cause of cancer-related mortality worldwide and accounts for greater than 800,000 deaths annually (1). *Helicobacter pylori* is the most common bacterial infection worldwide and represents the strongest known risk factor for the development of gastric adenocarcinoma. Pathologic outcomes of infection are mediated by complex interactions among bacterial virulence determinants, host constituents, and environmental factors. One *H. pylori* strain-specific virulence determinant is the *cag* pathogenicity island. *H. pylori* strains that harbor the *cag* island induce more severe gastric injury and augment the risk for gastric cancer compared to *cag*-negative strains (2). The *cag* island encodes a bacterial type IV secretion system (T4SS), which translocates the effector protein, CagA, into host cells. Intracellular CagA can become phosphorylated (3-5) or remain unphosphorylated; in either form, CagA aberrantly activates numerous signaling pathways which are altered in gastric cancer, resulting in cellular responses that lower the threshold for carcinogenesis (6-8). The *cag* T4SS can also translocate peptidoglycan (9), heptose bisphosphate (10, 11), and microbial DNA into host cells (12). However, only a subset of persons infected by *cag*-positive *H. pylori* strains ever develop cancer (13, 14), underscoring the importance of defining additional factors that increase gastric cancer risk.

Environmental conditions also modify the risk for carcinogenesis. Iron deficiency is associated with an increased risk for neoplasms that arise within the stomach and the intestinal tract (15-17). Our laboratory previously demonstrated that iron deficiency augments and accelerates the development of gastric carcinogenesis within the context of *H. pylori* infection in the Mongolian gerbil model, which was mediated, in part, by increased function of the *cag* T4SS (18). The gerbil model of infection recapitulates many features of *H. pylori*-induced gastric inflammation and carcinogenesis in humans (19, 20); however, due to the outbred nature of Mongolian gerbils, discerning the precise role of host responses to *H. pylori* within the context of iron deficiency in this model has been limited. Therefore, the aim of this study was to define the specific effects of iron deficiency on host mediators of *H. pylori*-induced gastric inflammation and injury in two well-defined, independent, genetically inbred murine models of *H. pylori* infection: wild-type C57BL/6 mice, and transgenic FVB/N INS-GAS mice that overexpress

gastrin and are genetically predisposed to develop gastric dysplasia (21, 22). One limitation of using C57BL/6 mice to study gastric carcinogenesis is that the development of premalignant lesions requires prolonged periods of *H. pylori* colonization within the stomach (>12 months). In contrast, male transgenic hypergastrinemic INS-GAS mice develop preneoplastic lesions (21-24), which parallel features of human carcinogenesis, as early as six weeks following *H. pylori* challenge. In humans, *H. pylori*-induced pangastritis leads to hypochlorhydria, which predisposes to the development of gastric cancer (25). *H. pylori* infection can also cause hypergastrinemia in humans, mediated either by cytokine-induced stimulation of gastrin (26) or as a result of a positive feedback loop following parietal cell loss and hypochlorhydria. INS-GAS mice contain a human gastrin transgene, which results in overexpression of gastrin, leading to gastric hyperplasia and hypoacidity, accompanied by a steady decline in parietal cell mass. As such, uninfected INS-GAS mice spontaneously develop atrophic gastritis, dysplasia, and gastric adenocarcinomas at approximately 20 months of age. Following infection with *H. pylori*, gastric carcinogenesis is accelerated (21-24). Thus, the INS-GAS murine model parallels human gastric pathophysiology with respect to hypochlorhydria and hypergastrinemia, and importantly, these mice develop advanced premalignant and malignant lesions, not typically observed in wild-type mice. Host inflammatory and metabolic alterations that occur within gastric mucosa in response to *H. pylori* under conditions of iron deficiency were defined in these murine models and subsequently validated in humans.

RESULTS

Iron deficiency augments *H. pylori*-induced gastric inflammation and injury in C57BL/6 and INS-GAS mice. We utilized two independent inbred murine models of *H. pylori* infection, wild-type C57BL/6 mice and transgenic hypergastrinemic INS-GAS mice, to precisely define the effects of iron deficiency on host responses within the context of *H. pylori* infection. Mice were maintained on iron-replete or iron-depleted diets, challenged with or without the wild-type *cag*-positive *H. pylori* strain PMSS1, and then euthanized eight weeks post-challenge (Supplemental Figure 1A). To assess the effectiveness of iron depletion, we performed complete blood counts (CBC) and assessed parameters of iron deficiency. Levels of hemoglobin (Supplemental Figure 2 and 3, A and B), hematocrit (Supplemental Figure 2 and 3, C and D), and mean corpuscular volume (Supplemental Figure 2 and 3, E and F) were significantly reduced among C57BL/6 and INS-GAS mice maintained on iron-depleted diets, compared to those maintained on iron-replete diets, and this occurred independent of *H. pylori* infection (Supplemental Figure 2 and 3). Further, *H. pylori* infection did not induce iron deficiency or exacerbate the iron deficiency observed in mice maintained on an iron-depleted diet (Supplemental Figure 3).

Since gastric pH may affect the reduction of ferric iron (Fe^{3+}) to ferrous iron (Fe^{2+}), which could in turn affect iron absorption and further exacerbate iron deficiency, we next assessed the gastric pH in *H. pylori*-infected INS-GAS mice maintained on iron-replete or iron-depleted diets. These data demonstrate that chronically infected mice, regardless of diet, harbor a gastric pH around 3-4 (data not shown), which suggests that iron would be available in a soluble and absorbable form and pH levels would not further exacerbate the iron deficiency observed in this model.

Having established iron deficiency in our murine models, we next assessed *H. pylori* colonization and the severity of gastric inflammation and injury. Consistent with our previous findings in the Mongolian gerbil model, *H. pylori* colonization was not altered under conditions of iron deficiency in C57BL/6 mice (Figure 1A). Further, *H. pylori* colonized the gastric antrum, transition zone, and corpus at similar levels in mice maintained on iron-replete or

iron-depleted diets (Figure 1B). Minimal infiltration of immune cells developed among uninfected mice maintained on either iron-replete (Figure 1, C and D, Supplemental Figure 4, A and E) or iron-depleted (Figure 1, C and E, Supplemental Figure 4, B and E) diets, while inflammatory infiltrates were significantly increased among *H. pylori*-infected C57BL/6 mice maintained on either diet (Figure 1, C, F and G, Supplemental Figure 4, C-E). When levels of acute and chronic inflammation were assessed independently, *H. pylori* induced significantly higher levels of acute (Figure 1H) and chronic (Figure 1I) inflammation compared to uninfected mice, and chronic inflammation was further augmented under conditions of iron deficiency (Figure 1I). No differences in total, acute, or chronic gastric inflammation were observed among uninfected C57BL/6 mice maintained on either diet (Figure 1, C-I, Supplemental Figure 4), indicating that iron deficiency augments gastric inflammation only within the context of *H. pylori* infection. To more rigorously assess the extent and severity of gastric inflammation among C57BL/6 mice, we quantitatively assessed levels of MPO (Figure 1J) and CD45 (Figure IK) by immunohistochemistry to enumerate neutrophils and macrophages (MPO) as well as leukocytes (CD45), respectively. These data parallel the inflammation scores and demonstrate that iron deficiency significantly augments the infiltration of immune cells and *H. pylori*-induced inflammation.

To validate and extend these findings into a more robust model of gastric carcinogenesis, INS-GAS mice were maintained on iron-replete or iron-depleted diets and then challenged with *H. pylori* strain PMSS1 (Supplemental Figure 1A). Similar to C57BL/6 mice, *H. pylori* colonization was not altered under conditions of iron deficiency (Figure 2A) and *H. pylori* colonized the gastric antrum, transition zone, and corpus at similar levels in mice maintained on iron-replete or iron-depleted diets (Figure 2B). *H. pylori* also induced significantly higher levels of total inflammation in INS-GAS mice maintained on iron-replete and iron-depleted diets, compared to uninfected controls, and this was significantly augmented under conditions of iron deficiency (Figure 2, C-G, Supplemental Figure 5).

When levels of acute and chronic inflammation were assessed independently, both acute (Figure 2H) and chronic (Figure 2I) inflammation were further exacerbated under iron-depleted conditions. Consistent with heighted levels of gastric inflammation among infected INS-GAS mice maintained on iron-depleted diets, the incidence of gastric dysplasia was also heightened, whereby 44% of infected mice maintained on iron-depleted diets developed gastric dysplasia, compared to 20% of infected mice maintained on iron-replete diets (Figure 2, J and K).

***H. pylori*-induced inflammation and injury under conditions of iron deficiency is reversible.** To assess whether *H. pylori*-induced inflammatory phenotypes observed under conditions of iron deficiency in INS-GAS mice could be reversed, two groups of mice were maintained on iron-depleted diets for two weeks prior to challenge with or without *H. pylori* strain PMSS1. One group was continued on an iron-depleted diet, while the other group was switched to an iron-replete diet two weeks post-challenge. Mice were then euthanized eight weeks post-challenge (Supplemental Figure 1B). Consistent with our previous findings, parameters of iron deficiency were significantly reduced among mice maintained on an iron-depleted diet, but were restored following the switch to an iron-replete diet (Figure 3A). *H. pylori* colonization density was similar among mice maintained on an iron-depleted diet compared to mice switched to an iron-replete diet (Figure 3B). Importantly, the severity of *H. pylori*-induced inflammation and injury was significantly reduced when mice were switched from an iron-depleted diet to an iron-replete diet (Figure 3, C and D), suggesting that these phenotypes are reversible following restoration of iron status.

***H. pylori* induces biased proinflammatory immune responses within the context of iron deficiency.** We next sought to define specific mechanisms that regulated iron-deficient phenotypes in a subset of C57BL/6 and INS-GAS mice by utilizing a 25-plex chemokine and cytokine panel. As expected, we observed a significant increase in levels of several proinflammatory chemokines and cytokines following *H. pylori* infection, some of which were further augmented under conditions of iron deficiency. Among C57BL/6 mice, KC (Figure 4A) and MIP-2 (Figure 4B), chemokines important in neutrophil recruitment, MIP-1α (Figure 4C) and MIP-1β (Figure 4D),

chemokines important for directing macrophage responses, and IP-10 (Figure 4E) and RANTES (Figure 4F), chemokines important in driving Th1 T cell responses, were significantly increased among infected mice under conditions of iron deficiency compared to infected mice on iron-replete diets. Several other cytokines were increased among infected C57BL/6 mice, but were not significantly altered by iron deficiency. These included IL-1α, IL-1β, IL-2, and IL-17 (Supplemental Figure 6). Among INS-GAS mice, MIP-1α (Figure 4G) and IL-17 (Figure 4H) were significantly increased among infected mice under conditions of iron deficiency compared to infected mice on iron-replete diets. Several other cytokines were also increased among INS-GAS mice infected with *H. pylori* independent of iron status, including IP-10, IL-1α, KC, INF-γ, MIP-2, IL-1β, IL-6, and IL-15 (Supplemental Figure 7).

In vivo-adaptation of *H. pylori* to conditions of iron deficiency does not alter *cag* T4SS function or *vacA* expression. We previously demonstrated that in vivo-adaptation of *H. pylori* to conditions of iron deficiency in Mongolian gerbils led to increased function of the *cag* T4SS, as assessed by CagA expression and translocation (18). Thus, to assess the effects of iron deficiency on *cag* T4SS function in mice, in vivo-adapted *H. pylori* strains were isolated from C57BL/6 and INS-GAS mice maintained on either iron-replete or iron-depleted diets. *H. pylori* strains were co-cultured with gastric epithelial cells and levels of CagA expression and CagA translocation, as measured by tyrosine phosphorylation, were assessed by Western blot analysis (Supplemental Figure 8). In contrast to Mongolian gerbils, in vivo-adapted strains isolated from either C57BL/6 or INS-GAS mice did not differ in their ability to express CagA (Supplemental Figure 8, A-D) or translocate CagA into host cells (Supplemental Figure 8, A, B, and E-H) following adaptation to either dietary condition.

To assess whether in vivo-adaptation to conditions of iron deficiency altered expression levels of another well characterized *H. pylori* virulence factor, vacuolating cytotoxin (*vacA*), in vivo-adapted *H. pylori* strains were isolated from C57BL/6 and INS-GAS mice maintained on either iron-replete or iron-depleted diets. RNA was extracted from minimally passaged, log phase *H. pylori* and *vacA* gene expression was assessed by qRT-PCR. In

vivo-adapted *H. pylori* strains isolated from either C57BL/6 (Supplemental Figure 9A) or INS-GAS (Supplemental Figure 9B) mice did not exhibit significant differences in *vacA* gene expression following adaptation to either dietary condition. Collectively, these results indicate that host-driven mechanisms may mediate iron-dependent phenotypes in mice.

The gastric microbiota is not a significant driver of the proinflammatory phenotypes among INS-GAS mice under iron deficiency. To first assess the potential effect of the gastrin transgene on the microbiota, gastric tissue was harvested from uninfected wild-type FVB/N mice and transgenic hypergastrinemic INS-GAS mice (Supplemental Figure 1C) for 16S rRNA gene sequencing and microbial community analysis. These data demonstrated that there were no differences in α-diversity (Supplemental Figure 10A) between FVB/N and INS-GAS mice, but subtle differences in β-diversity (Supplemental Figure 10B), which were driven by the differential abundance of a sole genus, *Turicibacter* (Supplemental Figure 10C). These data suggest that the gastrin transgene does not significantly alter the diversity of the gastric microbiota.

To address the potential effects of iron deficiency on the microbiota, gastric tissue was harvested from uninfected INS-GAS mice maintained on iron-replete or iron-depleted diets (Supplemental Figure 1C) for 16S rRNA gene sequencing and microbial community analysis. These data demonstrated that there are no differences in α-diversity (Supplemental Figure 10D) or β-diversity (Supplemental Figure 10E) between INS-GAS mice maintained on iron-replete versus iron-depleted diets, indicating that iron deficiency does not significantly or dramatically alter the diversity or the community structure of the gastric microbiota. Collectively, these data suggest that the gastric microbiota is likely not a significant driver of the proinflammatory phenotypes in INS-GAS mice observed under conditions of iron deficiency. However, we cannot definitely exclude a potential effect of individual species or microbial-derived metabolites in the gastric microbiota or the effect of the intestinal microbiota, which would require more in depth analysis and possibly long-term monocolonization studies.

***H. pylori* alters metabolic profiles in C57BL/6 and INS-GAS mice under conditions of iron deficiency.** To increase the mechanistic depth of our studies, we next performed untargeted metabolomics on gastric tissue isolated from uninfected or *H. pylori*-infected C57BL/6 and INS-GAS mice, maintained on either iron-replete or iron-depleted diets. A comprehensive list of identified gastric mucosal metabolites in C57BL/6 mice and INS-GAS mice are listed in Supplemental Tables 1 and 2, respectively. From these individual metabolites, four major metabolic pathways were predicted to be altered following infection with *H. pylori* in both models: arginine and polyamine metabolism, L-lysine and purine degradation, fatty acid metabolism, and bile acid metabolism. Based on previous data demonstrating that bile acids are linked to gastrointestinal malignancies (27-29), targeted bile acid analyses were subsequently performed in both C57BL/6 (Supplemental Figure 11) and INS-GAS (Figure 5) mice.

Among C57BL/6 mice, total bile acid levels were significantly increased following *H. pylori* infection under conditions of iron deficiency (Supplemental Figure 11A). However, there were no significant differences in variants of muricholic acid (MCA) or cholic acid (CA) following *H. pylori* infection under iron-replete or iron-depleted conditions (Supplemental Figure 11 B-H). TUDCA was significantly increased following *H. pylori* infection under conditions of iron deficiency (Supplemental Figure 11I), while THDCA was significantly increased following *H. pylori* infection under iron-replete conditions (Supplemental Figure 11J). There were no significant differences in deoxycholic acid (DCA, Supplemental Figure 11N).

Among INS-GAS mice with a predisposition for carcinogenesis, bile acid levels were minimally changed under iron-replete conditions, when uninfected mice were compared to mice infected with *H. pylori* (Figure 5). However, total bile acids were significantly increased under conditions of iron deficiency in conjunction with *H. pylori* infection (Figure 5A), similar to C57BL/6 mice. However, in contrast to C57BL/6 mice, variants of MCA, CA, and DCA were significantly increased by *H. pylori* under conditions of iron deficiency compared to infected mice under iron-replete conditions (Figure 5B-N). Collectively, these data indicate that iron deficiency, in

conjunction with *H. pylori* infection, is linked to altered bile acid metabolism in INS-GAS mice. These data raise the hypothesis that bile acids may mediate the increased gastric inflammation and injury observed in this model.

Deoxycholic acid treatment augments *H. pylori*-induced gastric inflammation and injury under iron-depleted conditions in INS-GAS mice. Bile acids regulate inflammation (30) and promote gastrointestinal malignancies, including premalignant and malignant lesions of the stomach (31-33). Deoxycholic acid (DCA) and other secondary bile acids have also been demonstrated to increase production of reactive oxygen species (ROS) and induce DNA damage, which increase the risk of carcinogenesis (34-36). To directly assess effects of the secondary bile acid DCA on the development of *H. pylori*-induced gastric inflammation and injury, INS-GAS mice were maintained on an iron-replete standard diet, challenged with or without *H. pylori*, and were then provided with water (H_2O) alone or water supplemented with 100 μM DCA (Supplemental Figure 1D). Of interest, *H. pylori*-infected mice consumed significantly more water than uninfected mice, but there were no differences in consumption of water alone versus water supplemented with 100 μM DCA (Figure 6A). Neither *H. pylori* infection nor consumption of water supplemented with 100 μM DCA led to differences in parameters of iron deficiency, including serum ferritin, hemoglobin, hematocrit, or mean corpuscular volume (Supplemental Figure 12). *H. pylori* colonization was significantly lower among mice receiving water supplemented with 100 μM DCA compared to water alone (Figure 6B). *H. pylori* significantly increased gastric inflammation among mice receiving water alone or water supplemented with DCA, compared to uninfected mice, and this was further augmented in mice receiving DCA (Figure 6C). Consistent with increased levels of inflammation, DCA also significantly increased the incidence of low-grade gastric dysplasia, compared to infected mice receiving water alone (40% versus 0%, Figure 6, D and E), suggesting that secondary bile acids, such as DCA, may exert a direct role in mediating *H. pylori*-induced inflammation and injury. Bacterial bile acid metabolism plays a key role in modulating innate immunity by controlling the balance of inflammatory T helper cells and anti-inflammatory T regulatory cells in intestinal tissue. Secondary bile acids have been shown to induce Tregs by increasing Foxp3 expression (37-39). Thus, we assessed the expression of Foxp3 by immunohistochemistry in

12

gastric tissue sections from uninfected and *H. pylori*-infected mice treated with or without DCA. These results demonstrate that *H. pylori* induces the expression of Foxp3 in gastric tissue, but DCA alone does not alter the abundance of Foxp3-positive cells in the stomach, suggesting that the presence of secondary bile acids may exacerbate gastric inflammation rather than promote an anti-inflammatory T regulatory response (Figure 6F).

Since DCA has been shown to induce secretion system function and virulence in other bacterial pathogens, such as *Shigella* (40), we next assessed the direct role of DCA on *H. pylori* Cag T4SS function. Gastric epithelial cells were co-cultured with *H. pylori* and either vehicle control or DCA and levels of CagA expression and translocation were assessed by Western blot analysis. These data demonstrate that *H. pylori* exposure to DCA induces a significant increase in translocation of CagA into host cells (Figure 6G-I), indicating that augmentation of Cag T4SS function is another mechanism regulating increased inflammation and injury by DCA under conditions of iron deficiency.

To assess and extend the role of *H. pylori* and DCA in an acute model of infection, 3D human gastric organoids were converted to 2D monolayers, co-cultured with or without *H. pylori*, and subsequently treated with or without DCA (Supplemental Figure 13). Compared to uninfected controls (Supplemental Figure 13A), *H. pylori* infection (Supplemental Figure 13B), DCA treatment (Supplemental Figure 13C), and the combination of *H. pylori* infection and DCA treatment (Supplemental Figure 13C) induced significantly increased levels of EGFR activation. *H. pylori* infection, DCA treatment, and the combination of *H. pylori* and DCA also induced significantly higher levels of IL-8 production and epithelial cell proliferation, compared to uninfected controls (Supplemental Figure 13, E and F). Collectively, these data indicate that DCA induces activation of proinflammatory and proliferative signaling pathways that may facilitate gastric carcinogenesis.

Bile acid sequestration significantly attenuates *H. pylori*-induced inflammation and injury under conditions of iron deficiency. To conversely assess the effects of a bile acid-sequestrant on the development of *H. pylori*-

induced gastric inflammation and injury under conditions of iron depletion, male INS-GAS mice were maintained on iron-replete or iron-depleted diets supplemented with or without 2% cholestyramine, challenged with or without *H. pylori*, and then euthanized eight weeks post-challenge (Supplemental Figure 1E). As expected, hemoglobin, hematocrit, and mean corpuscular volume (Figure 7A) levels were significantly reduced among *H. pylori*-infected mice maintained on iron-depleted diets with and without cholestyramine, compared to *H. pylori*-infected mice maintained on iron-replete diets with and without cholestyramine, and cholestyramine had no effect on parameters of iron deficiency (Supplemental Figure 14). To assess the effectiveness of cholestyramine treatment, targeted bile acid analysis was performed and demonstrated that cholestyramine treatment significantly reduced the secondary bile acid DCA in gastric tissue (Figure 7B). Mice exhibited similar levels of *H. pylori* colonization when maintained on iron-replete or iron-depleted diets, regardless of the presence of cholestyramine (Figure 7C).

Having confirmed the effectiveness of iron-depleted diets, we next assessed levels of gastric inflammation and injury. As expected, infection with *H. pylori* significantly increased gastric inflammation in mice under both iron-replete and iron-depleted conditions, compared to uninfected controls, and this was significantly augmented under conditions of iron deficiency (Figure 7D). Importantly, treatment with cholestyramine significantly reduced levels of *H. pylori*-induced gastric inflammation under conditions of iron deficiency (Figure 7D). Consistent with our previous findings (Figure 2F), iron deficiency increased the incidence of dysplasia among *H. pylori*-infected mice. However, consistent with reduced *H. pylori*-induced inflammation, cholestyramine treatment also significantly reduced the incidence of gastric dysplasia under conditions of iron deficiency (35% versus 5%, Figure 7, E and F). Collectively, these results suggest that bile acids augment *H. pylori*-induced inflammation and injury under conditions of iron deficiency in INS-GAS mice and that bile acid-reducing therapies may represent an effective means of controlling detrimental host responses.

Use of bile acid-sequestrants is associated with a reduced risk of gastric cancer in humans. To extend our in vivo studies into human populations and to test the hypothesis that decreased gastric mucosal exposure to bile acids is associated with a reduced risk of gastric cancer, we conducted a retrospective cohort analysis analyzing the association between bile acid-sequestrant medications and risk of incident gastric cancer. Using a national database containing electronic-health records with individual-level data (*N*~15 million), including fills of prescription medications and longitudinal medical follow-up, we constructed a cohort of individuals who had undergone testing for *H. pylori* (*N*=725,134). We selected this as the base cohort in order to limit selection and ascertainment bias, as well as to reduce residual confounding at inception. In this database, electronic health records are accurate and complete starting from the year 2000 onward. After exclusion of patients (see Supplemental Methods), the final analytic dataset included 416,885 patients. Date of study entry was defined as the date of *H. pylori* testing. Among those meeting full inclusion criteria for the analytic cohort, all completed prescription fills of bile acid-sequestrant medications in the five years prior to study entry through the last date of follow-up were captured for each patient (primary exposure). Cumulative exposure to bile acid-sequestrant medications was a continuous variable representing the proportion of total number of days exposed to bile acid-sequestrants. The total days exposed was determined by calculating the quantity dispensed for individual bile acid-sequestrant prescriptions filled. Specific bile acid-sequestrants included cholestyramine, colestipol, and colesevelam. The mean follow-up time for the cohort was 7.9 years (standard deviation (SD): four years). Therefore, including the five years prior to study entry, cumulative exposure to bile acid-sequestrants was captured over approximately 13 years for this analysis.

The demographics and clinical characteristics of the individuals comprising the analytic cohort are provided in Table 1. There were 19,634 (4.7%) individuals who had any exposure to bile acid-sequestrants at any time prior to study entry or during the follow-up period. As characteristic of veteran demographics, the majority of the cohort was male (89%) and non-Hispanic White (63%). Given the large size of the cohort (*N*=416,885), small differences in covariates between exposed and non-exposed groups, while statistically significant (Wilcoxon test

or Pearson Chi-squared test) may not be clinically significant. For example, a 1% difference in frequency of male sex and a 2% difference in *H. pylori* prevalence both are statistically significant based on the Pearson Chi-squared test *P* value<0.05, but these are likely not clinically significant differences. Compared to those with no exposure to bile acid-sequestrants, individuals with exposure tended to be slightly older (mean age (SD): 57 (14) versus 54 (16) years), slightly less often male (88% versus 89%), more often non-Hispanic White (70% versus 63%), more often smokers (44% versus 37%), and slightly less often *H. pylori* positive (32% versus 34%). Among 416,885 individuals, a total of 1,956 cases of gastric cancer occurred during follow-up. After adjusting for relevant confounders, bile acid-sequestrant use on 1% of the total days was associated with a significant 8% reduced risk of incident gastric cancer (adjusted hazard ratio, HR 0.92; 95% CI, 0.86-0.98; *P*<0.01; Table 2). This reduction in risk was greater with a larger proportion of total days exposed; exposure to bile acid-sequestrant on 5% of total days was associated with a significant 30% risk reduction (HR 0.70; 95% CI, 0.53-0.92; *P*=0.015; Table 2). This observation appeared to be maintained with increasing proportion of 20% days exposed (HR 0.71; 95% CI, 0.48-1.04; *P*=0.073; Table 2), although smaller sample size in this stratum limited power. When the reference category was bile acid-sequestrant exposure for 1% of total days (instead of no exposure), exposure on 5% of days was associated with a significant 24% reduced risk of incident gastric cancer (HR 0.76; 95% CI, 0.62-0.94; *P*<0.05; data not shown). When analyzed separately, cholestyramine exposure on 5% of total days compared to no exposure had a slightly greater protective effect (HR 0.51; 95% CI, 0.30-0.86; *P*<0.05; data not shown); however, the reduced sample size precludes strong conclusions. The suggestive protective effect of bile acid-sequestrants on risk of incident gastric cancer was also maintained irrespective of anatomic location of gastric cancer.

Expression of the bile acid receptor TGR5 parallels the severity of gastric disease in humans. TGR5 is an important bile acid receptor that regulates bile acid metabolism and mucosal immune homeostasis. TGR5 is expressed in parenchymal cells as well as hematopoietic cell lineages, and among bile acid receptors, TGR5 has the highest affinity for secondary bile acids (30, 41). Importantly, TGR5 has been shown to be highly expressed

in gastric cancer, with expression levels being associated with increased proliferation, migration, and epithelial-mesenchymal transition (42) and decreased patient survival (43). To further investigate the role of bile acid-mediated pathogenesis in humans and identify potentially druggable targets, levels of TGR5 in patients with varying disease pathologies across the cascade of gastric carcinogenesis were assessed using a human gastric tissue microarray. TGR5 expression paralleled the severity of gastric disease, with the highest levels present among patients with non-cardia gastric cancer (Figure 8A). There were no differences in TGR5 expression levels between diffuse versus intestinal-type gastric cancer (data not shown). TGR5 staining patterns increased in a step-wise manner from normal gastric tissue (Figure 8B) to multifocal atrophic gastritis without intestinal metaplasia (Figure 8C), to intestinal metaplasia (Figure 8D), to gastric cancer (Figure 8E). To validate these findings, we next assessed *TGR5* expression via qRT-PCR in normal human gastric tissue, gastric tissue with gastritis alone, and gastric tissue with adenocarcinoma (Table 3). These data corroborate our immunohistochemistry findings and demonstrate that *TGR5* gene expression levels parallel the severity of gastric lesions (Figure 8F).

To explore the role of *Tgr5* in *H. pylori*-induced gastric inflammation in mice in greater depth, wild-type C57BL/6 and *Tgr5⁻ᐟ⁻* homozygous littermates were challenged with Brucella broth, as an uninfected control, or with *H. pylori* strain PMSS1 and then euthanized eight weeks post-challenge (Supplemental Figure 1F). *H. pylori* colonization density (Supplemental Figure 15A) and levels of *H. pylori*-induced inflammation (Supplemental Figure 15B) were not significantly different among *H. pylori*-infected wild-type versus *Tgr5⁻ᐟ⁻* mice, indicating that TGR5 may either represent a biomarker for disease severity in humans or that TGR5 may exert different roles in promoting disease in humans and mice.

DISCUSSION

H. pylori induces detrimental host responses that lower the threshold for the development of gastric cancer. Using refined and tractable genetic models, we have demonstrated that *H. pylori* increases the severity of gastric inflammation and the development of premalignant lesions in the setting of iron deficiency, and this is, in part, mediated through altered bile acid production and a concomitant increase in levels of the secondary bile acid, deoxycholic acid, which has been associated with a variety of gastrointestinal cancers (27-29, 34). Treatment with deoxycholic acid directly contributes to and exacerbates *H. pylori*-induced inflammation and development of premalignant lesions, while targeted reduction of bile acids through treatment with cholestyramine significantly reduces *H. pylori*-induced inflammation and injury in the context of iron deficiency. Importantly, in a large human cohort with confirmed *H. pylori* testing, use of bile acid-sequestrant medications was associated with a significantly reduced risk of gastric cancer based on cumulative exposure over time. Although this correlation between bile acid-sequestrant use and risk of gastric cancer is important, there is a crucial need for this to be studied in the future in a more controlled fashion in a population with a higher incidence of gastric cancer.

Bile acids are present predominantly in the bile of mammals and are synthesized from cholesterol in the liver. Primary bile acids can be conjugated with glycine or taurine to form primary conjugated bile acids, which are then secreted via the bile duct into the duodenum, where they emulsify and solubilize lipid-soluble nutrients to facilitate digestion and absorption of cholesterol and lipids. In the colon, primary bile acids serve as substrate for bacterial biotransformation into secondary bile acids, such as deoxycholic acid and lithocholic acid, which can exert pathogenic effects under certain conditions. The majority of intestinal bile acids are reabsorbed from the terminal ileum and transported back to the liver through the process of enterohepatic recirculation. Previous reports demonstrate that high levels of bile acids are present in the gastric juice of normal subjects (44) and patients with ulcer disease (45). Further, the combination of bile reflux and acid reflux increases the risk of gastritis, which has been linked to gastric cancer in a recent large human cohort study (46). Another recent study characterized differences in gastric bile acid composition between patients with gastritis and healthy individuals

and demonstrated that although bile acids are present in the stomachs of healthy individuals and patients with non-bile acid reflux gastritis, conjugated bile acids were prominent components in gastric juice of patients with bile acid reflux gastritis (47). Collectively, these studies demonstrate that bile acid reflux occurs in patients with and without gastritis but increased levels of conjugated bile acids are associated with the risk for gastric carcinogenesis.

In addition to their role as dietary surfactants, bile acids serve as key signaling molecules in the modulation of epithelial cell proliferation, gene expression, and metabolism. However, when such homeostatic pathways are disrupted, bile acids can promote inflammation, metabolic disorders, and cancer. Specifically, secondary, hydrophobic bile acids function as tumor promoters for a variety of gastrointestinal cancers (27-29, 34) through a combination of mechanisms, including induction of direct oxidative stress with concomitant DNA damage, proliferation, apoptosis, epigenetic gene regulation, altered expression of bile acid receptors, and dysbiosis of the gut microbiota. The secondary bile acid, DCA, can induce activation of the transcription factor NF-κB, leading to increased inflammatory cytokine production, enhanced cell survival, and hyperproliferation in esophageal (48, 49), gastric (50), and colon (51) cancer cells. DCA can also induce cyclooxygenase-2 (COX-2) expression through transactivation of the epidermal growth factor receptor (EGFR) (52), which leads to inflammation and hyperproliferation in pancreatic (53) and squamous esophageal (54) cells. In addition to transactivation of EGFR, DCA can induce epithelial hyperproliferation through activation of extracellular signal-regulated kinase (ERK) and protein kinase C (PKC) signaling pathways (55) and can also activate β-catenin signaling, extracellular signal-regulated kinases 1 and 2 (ERK1/2) signaling via activator protein (AP1) and c-Myc-targeted pathways (56), stimulating cancer cell proliferation and invasiveness. In addition to direct interactions with transmembrane and nuclear signaling receptors on epithelial cells, bile acids also activate innate and adaptive immune cells to regulate mucosal immune responses (30, 57, 58). Our new data now reveal a previously unappreciated role that secondary bile acids may exert on *H. pylori* virulence, namely augmented function of the Cag type IV secretion system. Thus, dysregulation of bile acid homeostasis leads to activation of numerous deleterious host and microbial

signaling pathways directly involved in heightened proinflammatory responses and activation of signaling cascades that predispose to and promote carcinogenesis.

Bile acid-mediating signaling occurs through two primary bile acid receptors, FXR (farsenoid X receptor) and TGR5 (transmembrane G-protein-coupled bile acid receptor), both of which are important for regulating bile acid metabolism and mucosal immune homeostasis (30, 59). FXR is expressed on parenchymal cells, primarily hepatocytes and ileal IECs, while TGR5 is expressed on these cells as well as hematopoietic cell linages, most notably monocytes and macrophages. Importantly, TGR5 has the highest affinity for secondary bile acids (30, 41), and has been shown to be overexpressed in gastric adenocarcinomas and increased TGR5 expression levels are strongly associated with decreased patient survival (43). Further, overexpression of TGR5 is associated with increased proliferation, migration, and epithelial-mesenchymal transition (42). We have now demonstrated that TGR5 expression levels also significantly increase with advancing disease severity along the gastric carcinogenic cascade. The discovery of the role of bile acid receptors in a number of diseases, including cholangiocarcinoma, hepatocellular carcinoma, and colon cancer have led to the development of novel receptor agonists for potential treatments and therapies (41). Our data therefore indicate that, in addition to heightened levels of bile acids, TGR5 expression is increased in gastric carcinogenesis in humans and thus may be an important prognostic factor for gastric cancer. However, studies are needed to provide more direct evidence linking TGR5 receptor signaling to gastric carcinogenesis, such as those performed in animal models of *Tgr5*-deficincy that develop more advanced gastric disease in response to *H. pylori* infection.

In summary, our studies demonstrate that iron deficiency augments gastric carcinogenesis in the context of *H. pylori* infection and this is, in part, mediated through altered bile acid metabolism. These findings raise the intriguing possibility that targeting bile acid metabolic pathways and/or bile acid receptor signaling to reduce the levels of specific bile acids and accumulation of secondary bile acids as well as inhibiting activation of detrimental signaling pathways may be a novel and beneficial treatment strategy in gastric cancer prevention. Quantification

of levels of iron, detrimental secondary bile acids, and bile acid receptors among *H. pylori*-infected individuals may also be useful in identifying subjects at high-risk for the progression to gastric cancer.

METHODS

Murine models of iron deficiency and *H. pylori* infection. Male and female wild-type C57BL/6 (Envigo) and male transgenic hypergastrinemic INS-GAS^{+/+} mice on a FVB/N background (21-24) were bred and housed in the Vanderbilt University Medical Center animal care facilities in a room with a 12-hour light-dark cycle at 21-22°C. Rodent diets were modified from TestDiet® AIN-93M (Purina Feed, LLC) to contain 0 ppm iron (iron-depleted, TestDiet® 5TWD) or 250 ppm iron (iron-replete, TestDiet® 5STQ). Mice were maintained on modified diets for two weeks prior to challenge with *H. pylori* and throughout the duration of the experiments. The wild-type *cag*-positive *H. pylori* strain PMSS1 was minimally passaged on trypticase soy agar plates with 5% sheep blood (TSA/SB, BD Biosciences) and in Brucella broth (BD Biosciences) supplemented with 10% fetal bovine serum (Atlanta Biologicals) for sixteen hours at 37°C with 5% CO_2. Mice were orogastrically challenged with Brucella broth, as an uninfected (UI) negative control, or with wild-type *cag*-positive *H. pylori* strain PMSS1 (Supplemental Figure 1A). For the diet reversal experiment, two groups of male INS-GAS mice were maintained on an iron-depleted diet two weeks prior to challenge with *H. pylori*. Mice were then challenged with Brucella broth or with wild-type *cag*-positive *H. pylori* strain PMSS1. Two weeks post-challenge, one group of mice was continued on an iron-depleted diet, while the other group of mice was switched to an iron-replete diet. Mice were euthanized eight weeks post-challenge (Supplemental Figure 1B). To assess the potential effect of the gastrin transgene on the gastric microbiota, gastric tissue was harvested from uninfected male FVB/N (Envigo) and INS-GAS mice co-housed for eight weeks (Supplemental Figure 1C). To assess the potential effect of iron deficiency on the gastric microbiota, gastric tissue was harvested from uninfected male INS-GAS mice that were co-housed and then maintained on an iron-replete or iron-depleted diet for eight weeks (Supplemental Figure 1C). For deoxycholic acid (DCA) treatment, male INS-GAS mice were maintained on an iron-replete standard rodent diet (LabDiet, PicoLab® Laboratory Rodent Diet, 5L0D*) and then orogastrically challenged with Brucella broth or with *H. pylori* strain PMSS1. Two weeks following challenge, mice were provided water alone or water supplemented with 100 μM DCA (Sigma-Aldrich) and mice were euthanized six weeks post-challenge (Supplemental Figure 1D). For cholestyramine-mediated bile acid suppression, male INS-GAS mice were

maintained on iron-replete or iron-depleted diets with or without 2% cholestyramine (Sigma-Aldrich, w/w) for two weeks prior to challenge with *H. pylori* and throughout the course of the experiment. Mice were then orogastrically challenged with Brucella broth or with *H. pylori* strain PMSS1 and euthanized eight weeks post-challenge (Supplemental Figure 1E). All animal studies were conducted in accordance with the Vanderbilt University Medical Center Institutional Animal Care and Use Committee (IACUC).

Histopathology. Linear strips of gastric tissue, extending from the squamocolumnar junction through the proximal duodenum, were fixed in 10% neutral-buffered formalin (Azer Scientific), paraffin-embedded, and stained with hematoxylin and eosin. A pathologist, blinded to treatment groups, assessed indices of inflammation and incidence of gastric injury, including gastric dysplasia. Severity of acute and chronic inflammation was graded 0-3 in both the gastric antrum and corpus, as previously described (18), for a cumulative score of 0-12. Dysplasia was graded as indefinite dysplasia (borderline nuclear and architectural epithelial changes that do not completely fit the patterns of dysplasia), low-grade dysplasia, or high-grade dysplasia.

Immunohistochemistry. To assess Foxp3 protein expression in mice, immunohistochemistry (IHC) analysis was performed on formalin-fixed, paraffin-embedded (FFPE) gastric tissue from INS-GAS mice using a rat monoclonal anti-Foxp3 antibody (Invitrogen 14-577-82). Numbers of Foxp3-positive cells were counted in five high-powered fields (HPF, 400X) with the highest counts in each mouse, and the average number of Foxp3-positive cells per HPF are shown. To assess myeloperoxidase (MPO) and CD45 protein expression in mice, IHC analysis was performed on FFPE gastric tissue from C57BL/6 mice using a rabbit polyclonal anti-MPO (prediluted, Biocare Medical PP023AA) and anti-CD45 (Abcam ab10558) antibody, respectively. Numbers of MPO- and CD45-positive cells were enumerated throughout the entire length of the mucosa and submucosa in each mouse, and quantified as numbers of positive cells per square mm of mucosa and submucosa. OuPath software was used to assist with the analysis of digital images of entire slides (60). To assess TGR5 protein expression in humans, IHC analysis was performed on a gastric cancer tissue microarray (TMA) using a rabbit

polyclonal anti-GPCR TGR5 antibody (Abcam ab72608). The gastric cancer TMA was generated at Vanderbilt University Medical Center with tissues from the Cooperative Human Tissue Network. A single pathologist scored TGR5 IHC staining in the gastric sections. The percentage of positive cells was assessed and the intensity of epithelial staining was graded on a scale of 0-3 (absent (0), weak (1), moderate (2), or strong (3)). Immunohistochemistry data are represented as TGR5 IHC scores, which were determined by multiplying the staining intensity by the percentage of positively stained cells, as previously described (61).

Statistics. Mean values are shown with standard error of the mean, scatter dot plots are shown with mean values, and box-and-whisker plots are shown with median values with whiskers designating minimum and maximum values. Unpaired parametric t-tests, one-way ordinary ANOVA with Sidak's multiple comparison tests, Chi-square and Fisher's exact tests were used for statistical comparisons. No samples were excluded from the analyses. All statistical analyses were performed using GraphPad Prism and a P value less than 0.05 was considered statistically significant. The following asterisks designations reflect the following P values: ****, $P<0.0001$; ***, $P<0.001$; **, $P<0.01$; *, $P<0.05$. NS designates not statistically significant.

For the human retrospective cohort analysis, descriptive characteristics of individuals with bile acid-sequestrant exposure versus non-exposure were generated and then compared using Pearson's Chi-squared test for categorical variables and Wilcoxon test for continuous variables. The date of study entry (T_0, time zero) was defined as the date of *H. pylori* testing. Individuals were followed until the earliest of the following events: incident gastric cancer diagnosis (primary outcome), death, loss to follow-up, or end of study period (May 31, 2020). Multivariable Cox regression analysis was performed to estimate the association between cumulative bile acid medication exposure and risk of incident gastric cancer. Secondary analyses of individual bile acid-sequestrant medications as the primary exposure were performed, and secondary analyses with the primary outcome as incident gastric cancer according to anatomic location were also conducted. We generated three categories of cumulative exposure based on the distribution of individuals' proportion of total days of exposure to bile acid-

sequestrant medications (continuous variable) in order to assess whether the association with risk of gastric cancer changed according to magnitude of cumulative exposure. These categories were graded as 1% of total days exposed to 5% of total days exposed to >20% of total days exposed. Analyses were adjusted for relevant confounders, including age, sex, race/ethnicity, smoking, and *H. pylori* status. All statistical analyses were performed using Stata 15 and R. Statistical significance was set at a two-tailed *P* value<0.05.

Study approval. All animal and human studies were conducted in accordance with the Declaration of Helsinki principles and have been approved by the Vanderbilt University Medical Center Institutional Animal Care and Use Committee (IACUC) and the Vanderbilt University Medical Center Institutional Review Board (IRB), respectively. The human retrospective cohort analysis was approved under IRB #145579 under the category of exempt studies (minimal risk). This was a retrospective analysis of already existing data and no new human data were generated for this study, nor were any patients contacted. Human gastric tissue samples used for qRT-PCR were acquired from the Cooperative Human Tissue Network and these analyses were approved under IRB #210729 under the category of a non-human subject study.

AUTHOR CONTRIBUTIONS

JMN designed research study, conducted experiments, acquired data, analyzed and interpreted data, wrote and edited manuscript.

MBP scored histologic and IHC data and edited manuscript.

SCS designed human retrospective cohort analysis, acquired, analyzed, and interpreted human cohort analysis data, wrote human cohort analysis sections, and edited manuscript.

JRG conducted animal breeding, genotyping, assisted with animal experiments, and edited manuscript.

JLH conducted DNA extractions for microbiota experiments.

CD conducted bioinformatic analysis for microbiota experiments and wrote microbiota methods.

JDC conducted untargeted metabolomics experiments, analyzed untargeted metabolomic data, edited manuscript.

AGD performed immunohistochemistry.

AH & RG analyzed and interpreted human cohort data.

LEW conducted gastric organoid experiments, acquired and analyzed organoid data, and edited manuscript.

AS conducted and assisted with Western blot experiments.

MMA conducted and assisted with Luminex chemokine and cytokine assays, provided reagents, and edited manuscript.

KTW assisted with Luminex chemokine and cytokine data analyses, provided reagents, and edited manuscript.

MKW designed human gastric tissue microarray through the Cooperative Human Tissue Network.

MWC assisted with untargeted metabolomics experiments, analyzed untargeted metabolomic data, wrote untargeted metabolomics methods, and edited manuscript.

KLS assisted with untargeted metabolomics experiments and edited manuscript.

BPC provided wild-type C57BL/6 and $Tgr5^{-/-}$ mice and edited manuscript.

CRF conducted targeted bile acid experiments, acquired targeted bile acid data, and edited manuscript.

JPZ oversaw DNA extractions, 16S rRNA gene sequencing, bioinformatic analysis for microbiota experiments, wrote microbiota methods, and edited manuscript.

RMP designed research study, directed experiments and aided in data interpretation, assisted with writing manuscript, and edited manuscript.

ACKNOWLEDGEMENTS

REFERENCES

1. Bray F, Ferlay J, Soerjomataram I, Siegel RL, Torre LA, and Jemal A. Global cancer statistics 2018: GLOBOCAN estimates of incidence and mortality worldwide for 36 cancers in 185 countries. *CA Cancer J Clin*. 2018;68(6):394-424.

2. Polk DB, and Peek RM, Jr. *Helicobacter pylori*: gastric cancer and beyond. *Nat Rev Cancer*. 2010;10(6):403-14.

3. Stein M, Bagnoli F, Halenbeck R, Rappuoli R, Fantl WJ, and Covacci A. c-Src/Lyn kinases activate *Helicobacter pylori* CagA through tyrosine phosphorylation of the EPIYA motifs. *Mol Microbiol*. 2002;43(4):971-80.

4. Tammer I, Brandt S, Hartig R, Konig W, and Backert S. Activation of Abl by *Helicobacter pylori*: a novel kinase for CagA and crucial mediator of host cell scattering. *Gastroenterology*. 2007;132(4):1309-19.

5. Mueller D, Tegtmeyer N, Brandt S, Yamaoka Y, De Poire E, Sgouras D, et al. c-Src and c-Abl kinases control hierarchic phosphorylation and function of the CagA effector protein in Western and East Asian *Helicobacter pylori* strains. *J Clin Invest*. 2012;122(4):1553-66.

6. Odenbreit S, Puls J, Sedlmaier B, Gerland E, Fischer W, and Haas R. Translocation of *Helicobacter pylori* CagA into gastric epithelial cells by type IV secretion. *Science*. 2000;287(5457):1497-500.

7. Amieva MR, Vogelmann R, Covacci A, Tompkins LS, Nelson WJ, and Falkow S. Disruption of the epithelial apical-junctional complex by *Helicobacter pylori* CagA. *Science*. 2003;300(5624):1430-4.

8. Franco AT, Israel DA, Washington MK, Krishna U, Fox JG, Rogers AB, et al. Activation of beta-catenin by carcinogenic *Helicobacter pylori*. *Proc Natl Acad Sci U S A*. 2005;102(30):10646-51.

9. Viala J, Chaput C, Boneca IG, Cardona A, Girardin SE, Moran AP, et al. Nod1 responds to peptidoglycan delivered by the *Helicobacter pylori* cag pathogenicity island. *Nat Immunol*. 2004;5(11):1166-74.

10. Stein SC, Faber E, Bats SH, Murillo T, Speidel Y, Coombs N, et al. *Helicobacter pylori* modulates host cell responses by Cag T4SS-dependent translocation of an intermediate metabolite of LPS inner core heptose biosynthesis. *PLoS Pathog*. 2017;13(7):e1006514.

11. Gall A, Gaudet RG, Gray-Owen SD, and Salama NR. TIFA Signaling in gastric epithelial cells initiates the Cag type 4 secretion system-dependent innate immune response to *Helicobacter pylori* infection. *MBio*. 2017;8(4):e01168-17.

12. Varga MG, Shaffer CL, Sierra JC, Suarez G, Piazuelo MB, Whitaker ME, et al. Pathogenic *Helicobacter pylori* strains translocate DNA and activate TLR9 via the cancer-associated Cag type IV secretion system. *Oncogene*. 2016;35(48):6262-9.

13. Atherton JC, and Blaser MJ. Coadaptation of *Helicobacter pylori* and humans: ancient history, modern implications. *J Clin Invest*. 2009;119(9):2475-87.

14. Blaser MJ, and Berg DE. *Helicobacter pylori* genetic diversity and risk of human disease. *J Clin Invest*. 2001;107(7):767-73.

15. Pra D, Rech Franke SI, Pegas Henriques JA, and Fenech M. A possible link between iron deficiency and gastrointestinal carcinogenesis. *Nutr Cancer*. 2009;61(4):415-26.

16. Akiba S, Neriishi K, Blot WJ, Kabuto M, Stevens RG, Kato H, et al. Serum ferritin and stomach cancer risk among a Japanese population. *Cancer*. 1991;67(6):1707-12.

17. Nomura A, Chyou PH, and Stemmermann GN. Association of serum ferritin levels with the risk of stomach cancer. *Cancer Epidemiol Biomarkers Prev*. 1992;1(7):547-50.

18. Noto JM, Gaddy JA, Lee JY, Piazuelo MB, Friedman DB, Colvin DC, et al. Iron deficiency accelerates *Helicobacter pylori*-induced carcinogenesis in rodents and humans. *J Clin Invest*. 2013;123(1):479-92.

19. Honda S, Fujioka T, Tokieda M, Satoh R, Nishizono A, and Nasu M. Development of *Helicobacter pylori*-induced gastric carcinoma in Mongolian gerbils. *Cancer Res*. 1998;58(19):4255-9.

20. Watanabe T, Tada M, Nagai H, Sasaki S, and Nakao M. *Helicobacter pylori* infection induces gastric cancer in Mongolian gerbils. *Gastroenterology*. 1998;115(3):642-8.

21. Wang TC, Koh TJ, Varro A, Cahill RJ, Dangler CA, Fox JG, et al. Processing and proliferative effects of human progastrin in transgenic mice. *J Clin Invest*. 1996;98(8):1918-29.

22. Wang TC, Dangler CA, Chen D, Goldenring JR, Koh T, Raychowdhury R, et al. Synergistic interaction between hypergastrinemia and *Helicobacter* infection in a mouse model of gastric cancer. *Gastroenterology*. 2000;118(1):36-47.

23. Fox JG, Wang TC, Rogers AB, Poutahidis T, Ge Z, Taylor N, et al. Host and microbial constituents influence *Helicobacter pylori*-induced cancer in a murine model of hypergastrinemia. *Gastroenterology*. 2003;124(7):1879-90.

24. Fox JG, Rogers AB, Ihrig M, Taylor NS, Whary MT, Dockray G, et al. *Helicobacter pylori*-associated gastric cancer in INS-GAS mice is gender specific. *Cancer Res*. 2003;63(5):942-50.

25. Uemura N, Okamoto S, Yamamoto S, Matsumura N, Yamaguchi S, Yamakido M, et al. *Helicobacter pylori* infection and the development of gastric cancer. *N Engl J Med*. 2001;345(11):784-9.

26. Weigert N, Schaffer K, Schusdziarra V, Classen M, and Schepp W. Gastrin secretion from primary cultures of rabbit antral G cells: stimulation by inflammatory cytokines. *Gastroenterology*. 1996;110(1):147-54.

27. Debruyne PR, Bruyneel EA, Li X, Zimber A, Gespach C, and Mareel MM. The role of bile acids in carcinogenesis. *Mutat Res*. 2001;480-481:359-69.

28. Bernstein H, Bernstein C, Payne CM, and Dvorak K. Bile acids as endogenous etiologic agents in gastrointestinal cancer. *World J Gastroenterol*. 2009;15(27):3329-40.

29. Di Ciaula A, Wang DQ, Molina-Molina E, Lunardi Baccetto R, Calamita G, Palmieri VO, et al. Bile acids and cancer: Direct and environmental-dependent effects. *Ann Hepatol*. 2017;16(Suppl. 1):s87-s105.

30. Chen ML, Takeda K, and Sundrud MS. Emerging roles of bile acids in mucosal immunity and inflammation. *Mucosal Immunol*. 2019;12(4):851-61.

31. Tatsugami M, Ito M, Tanaka S, Yoshihara M, Matsui H, Haruma K, et al. Bile acid promotes intestinal metaplasia and gastric carcinogenesis. *Cancer Epidemiol Biomarkers Prev*. 2012;21(11):2101-7.

32. Matsuhisa T, and Tsukui T. Relation between reflux of bile acids into the stomach and gastric mucosal atrophy, intestinal metaplasia in biopsy specimens. *J Clin Biochem Nutr*. 2012;50(3):217-21.

33. Matsuhisa T, Arakawa T, Watanabe T, Tokutomi T, Sakurai K, Okamura S, et al. Relation between bile acid reflux into the stomach and the risk of atrophic gastritis and intestinal metaplasia: a multicenter study of 2283 cases. *Dig Endosc*. 2013;25(5):519-25.

34. Bernstein H, Bernstein C, Payne CM, Dvorakova K, and Garewal H. Bile acids as carcinogens in human gastrointestinal cancers. *Mutat Res*. 2005;589(1):47-65.

35. Tsuei J, Chau T, Mills D, and Wan YJ. Bile acid dysregulation, gut dysbiosis, and gastrointestinal cancer. *Exp Biol Med*. 2014;239(11):1489-504.

36. Ajouz H, Mukherji D, and Shamseddine A. Secondary bile acids: an underrecognized cause of colon cancer. *World J Surg Oncol*. 2014;12:164.

37. Hang S, Paik D, Yao L, Kim E, Trinath J, Lu J, et al. Bile acid metabolites control TH17 and Treg cell differentiation. *Nature*. 2019;576(7785):143-8.

38. Song X, Sun X, Oh SF, Wu M, Zhang Y, Zheng W, et al. Microbial bile acid metabolites modulate gut RORgamma(+) regulatory T cell homeostasis. *Nature*. 2020;577(7790):410-5.

39. Campbell C, McKenney PT, Konstantinovsky D, Isaeva OI, Schizas M, Verter J, et al. Bacterial metabolism of bile acids promotes generation of peripheral regulatory T cells. *Nature*. 2020;581(7809):475-9.

40. Chiang IL, Wang Y, Fujii S, Muegge BD, Lu Q, Tarr PI, et al. Biofilm formation and virulence of *Shigella flexneri* are modulated by pH of gastrointestinal tract. *Infect Immun*. 2021;89(11):e0038721.

41. Schaap FG, Trauner M, and Jansen PL. Bile acid receptors as targets for drug development. *Nat Rev Gastroenterol Hepatol*. 2014;11(1):55-67.

42. Carino A, Graziosi L, D'Amore C, Cipriani S, Marchiano S, Marino E, et al. The bile acid receptor GPBAR1 (TGR5) is expressed in human gastric cancers and promotes epithelial-mesenchymal transition in gastric cancer cell lines. *Oncotarget*. 2016;7(38):61021-35.

43. Cao W, Tian W, Hong J, Li D, Tavares R, Noble L, et al. Expression of bile acid receptor TGR5 in gastric adenocarcinoma. *Am J Physiol Gastrointest Liver Physiol*. 2013;304(4):G322-7.

44. Collins BJ, Watt PC, O'Reilly T, McFarland RJ, and Love AH. Measurement of total bile acids in gastric juice. *J Clin Pathol*. 1984;37(3):313-6.

45. Rydning A, and Berstad A. Intragastric bile acid concentrations in healthy subjects and in patients with gastric and duodenal ulcer and the influence of fiber-enriched wheat bran in patients with gastric ulcer. *Scand J Gastroenterol*. 1985;20(7):801-4.

46. Li D, Zhang J, Yao WZ, Zhang DL, Feng CC, He Q, et al. The relationship between gastric cancer, its precancerous lesions and bile reflux: A retrospective study. *J Dig Dis*. 2020;21(4):222-9.

47. Zhao A, Wang S, Chen W, Zheng X, Huang F, Han X, et al. Increased levels of conjugated bile acids are associated with human bile reflux gastritis. *Sci Rep*. 2020;10(1):11601.

48. Kazumori H, Ishihara S, Rumi MA, Kadowaki Y, and Kinoshita Y. Bile acids directly augment caudal related homeobox gene Cdx2 expression in oesophageal keratinocytes in Barrett's epithelium. *Gut*. 2006;55(1):16-25.

49. Jenkins GJ, Cronin J, Alhamdani A, Rawat N, D'Souza F, Thomas T, et al. The bile acid deoxycholic acid has a non-linear dose response for DNA damage and possibly NF-kappaB activation in oesophageal cells, with a mechanism of action involving ROS. *Mutagenesis*. 2008;23(5):399-405.

50. Redlak MJ, Power JJ, and Miller TA. Prevention of deoxycholate-induced gastric apoptosis by aspirin: roles of NF-kappaB and PKC signaling. *J Surg Res*. 2008;145(1):66-73.

51. Payne CM, Bernstein C, Dvorak K, and Bernstein H. Hydrophobic bile acids, genomic instability, Darwinian selection, and colon carcinogenesis. *Clin Exp Gastroenterol*. 2008;1:19-47.

52. Cheng K, and Raufman JP. Bile acid-induced proliferation of a human colon cancer cell line is mediated by transactivation of epidermal growth factor receptors. *Biochem Pharmacol*. 2005;70(7):1035-47.

53. Tucker ON, Dannenberg AJ, Yang EK, and Fahey TJ, 3rd. Bile acids induce cyclooxygenase-2 expression in human pancreatic cancer cell lines. *Carcinogenesis*. 2004;25(3):419-23.

54. Roman S, Petre A, Thepot A, Hautefeuille A, Scoazec JY, Mion F, et al. Downregulation of p63 upon exposure to bile salts and acid in normal and cancer esophageal cells in culture. *Am J Physiol Gastrointest Liver Physiol*. 2007;293(1):G45-53.

55. Degirolamo C, Modica S, Palasciano G, and Moschetta A. Bile acids and colon cancer: Solving the puzzle with nuclear receptors. *Trends Mol Med*. 2011;17(10):564-72.

56. Pai R, Tarnawski AS, and Tran T. Deoxycholic acid activates beta-catenin signaling pathway and increases colon cell cancer growth and invasiveness. *Mol Biol Cell*. 2004;15(5):2156-63.

57. Inagaki T, Moschetta A, Lee YK, Peng L, Zhao G, Downes M, et al. Regulation of antibacterial defense in the small intestine by the nuclear bile acid receptor. *Proc Natl Acad Sci U S A*. 2006;103(10):3920-5.

58. Zhu C, Fuchs CD, Halilbasic E, and Trauner M. Bile acids in regulation of inflammation and immunity: Friend or foe? *Clin Exp Rheumatol*. 2016;34(4 Suppl 98):25-31.

59. Jia W, Xie G, and Jia W. Bile acid-microbiota crosstalk in gastrointestinal inflammation and carcinogenesis. *Nat Rev Gastroenterol Hepatol*. 2018;15(2):111-28.

60. Bankhead P, Loughrey MB, Fernandez JA, Dombrowski Y, McArt DG, Dunne PD, et al. QuPath: Open source software for digital pathology image analysis. *Sci Rep*. 2017;7(1):16878.

61. Noto JM, Rose KL, Hachey AJ, Delgado AG, Romero-Gallo J, Wroblewski LE, et al. Carcinogenic *Helicobacter pylori* strains selectively dysregulate the in vivo gastric proteome, which may be associated with stomach cancer progression. *Mol Cell Proteomics*. 2019;18(2):352-71.
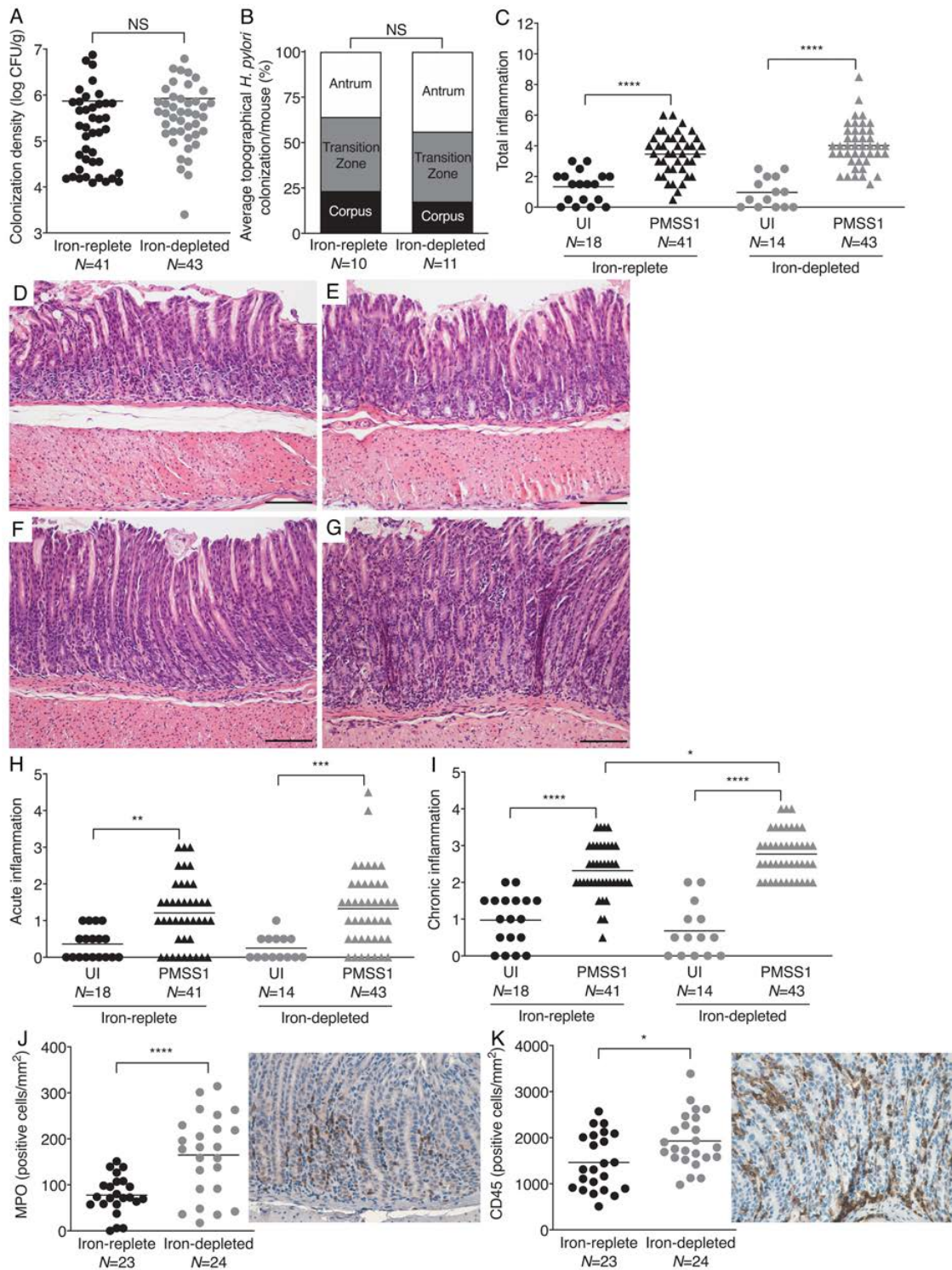
Figure 1. Iron deficiency augments *H. pylori*-induced chronic gastric inflammation in C57BL/6 mice. Wild-type male and female C57BL/6 mice were maintained on iron-replete (*N*=59) or iron-depleted (*N*=57) diets and then challenged with Brucella broth (UI) or *H. pylori* strain PMSS1. Mice were euthanized eight weeks post-

challenge. (**A**) Gastric tissue was homogenized and plated for quantitative culture. Colonization density is expressed as log colony-forming units/gram of tissue. (**B**) Gastric tissue was fixed, paraffin-embedded, and stained with a modified Steiner stain. The percentage of *H*. *pylori* colonizing the antrum, transition zone, and corpus was assessed and average topographical *H*. *pylori* colonization density/mouse is shown. (**C-I**) Gastric tissue was fixed, paraffin-embedded, and stained with hematoxylin and eosin. Levels of total gastric inflammation (0-12) were assessed (**C**). (**D-G**) Representative histologic images from antrum of uninfected mice maintained on iron-replete (**D**) or iron-depleted (**E**) diets and *H*. *pylori*-infected mice maintained on iron-replete (**F**) or iron-depleted (**G**) diets are shown (200X). Tissue sections were scored separately for acute (0-6) (**H**) and chronic gastric inflammation (0-6) (**I**). Levels of MPO (**J**) and CD45 (**K**) were assessed by IHC to enumerate neutrophils and macrophages (MPO) and leukocytes (CD45), respectively. Representative images are shown (400X). Each point represents data from an individual animal from three independent experiments. Mean values are shown in scatter dot plots. Scale bars represent 100 microns. Unpaired parametric t (**A-B**, **J-K**) and one-way ordinary ANOVA with Sidak's multiple comparisons (**C**, **H-I**) tests were used to determine statistical significance. ****, $P<0.0001$; ***, $P<0.001$; **, $P<0.01$; *, $P<0.05$; NS, not statistically significant.
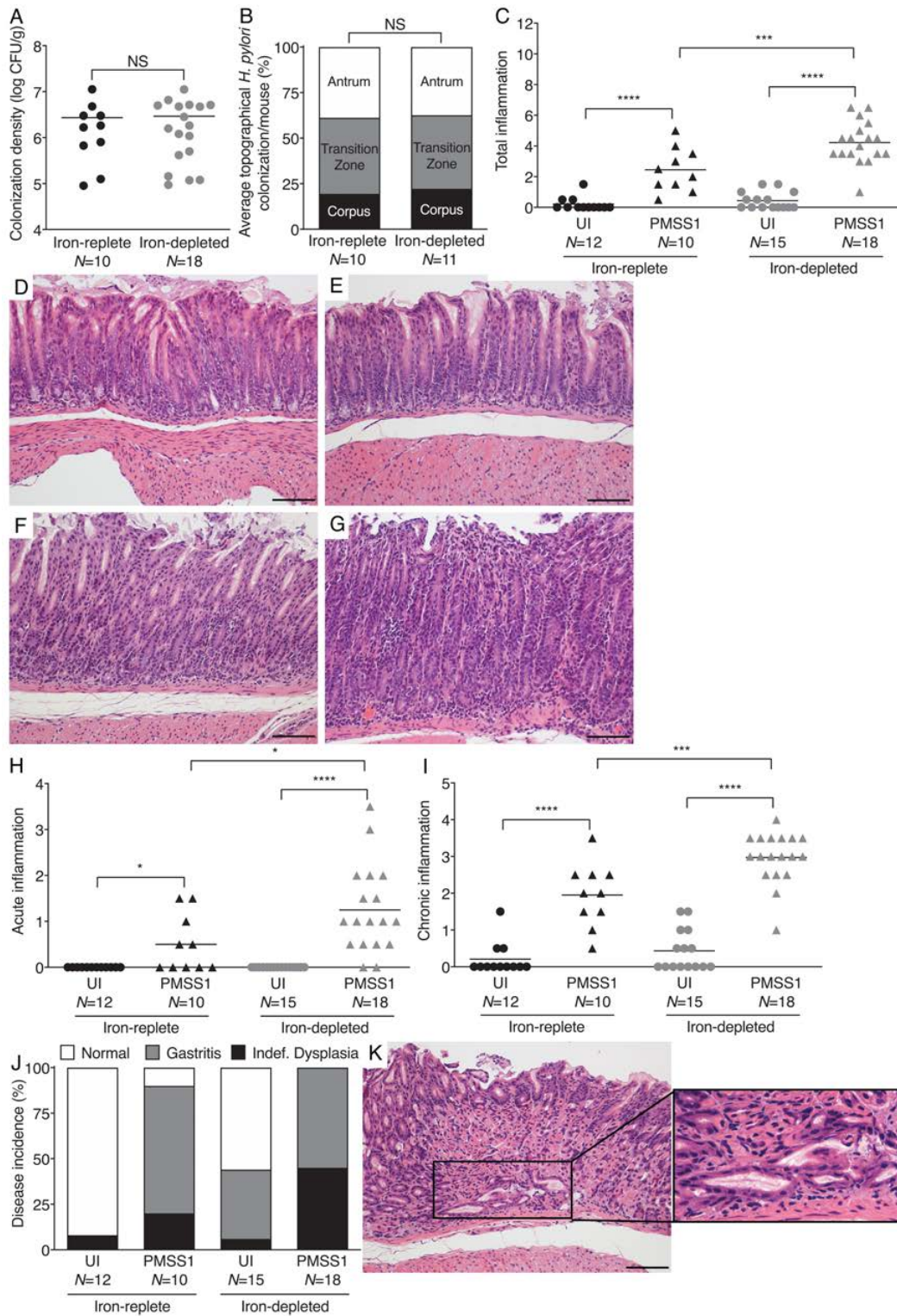
Figure 2. Iron deficiency augments *H. pylori*-induced gastric inflammation and injury in INS-GAS mice.

Male INS-GAS mice were maintained on iron-replete (*N*=22) or iron-depleted (*N*=33) diets and then challenged

with Brucella broth (UI) or *H. pylori* strain PMSS1. Mice were euthanized eight weeks post-challenge. (**A**) Gastric

tissue was homogenized and plated for quantitative culture. Colonization density is expressed as log colony-forming units/gram of tissue. (**B**) Gastric tissue was fixed, paraffin-embedded, and stained with a modified Steiner stain. The percentage of *H. pylori* colonizing the antrum, transition zone, and corpus was assessed and average topographical *H. pylori* colonization density/mouse is shown. (**C-K**) Gastric tissue was fixed, paraffin-embedded, and stained with hematoxylin and eosin. (**C**) Levels of total gastric inflammation (0-12) were assessed. (**D-G**) Representative histologic images from the antrum of uninfected mice maintained on iron-replete (**D**) or iron-depleted (**E**) diets and *H. pylori*-infected mice maintained on iron-replete (**F**) or iron-depleted (**G**) diets are shown (200X). Gastric tissue was scored separately for acute (**H**) and chronic (**I**) inflammation, and disease incidence (**J**). Dysplasia was graded as indefinite dysplasia (borderline nuclear and architectural epithelial changes that do not completely fit the patterns of dysplasia), low-grade or high-grade dysplasia. (**K**) Representative histologic images of indefinite dysplasia are shown (200X and 400X). Each point represents data from an individual animal from three independent experiments. Mean values are shown in scatter dot plots. Scale bars represent 100 microns. Unpaired parametric t (**A-B**), one-way ordinary ANOVA with Sidak's multiple comparisons (**C**, **H-I**), and Fisher's exact (**J**) tests were used to determine statistical significance. ****, $P<0.0001$; ***, $P<0.001$; *, $P<0.05$; NS, not statistically significant.
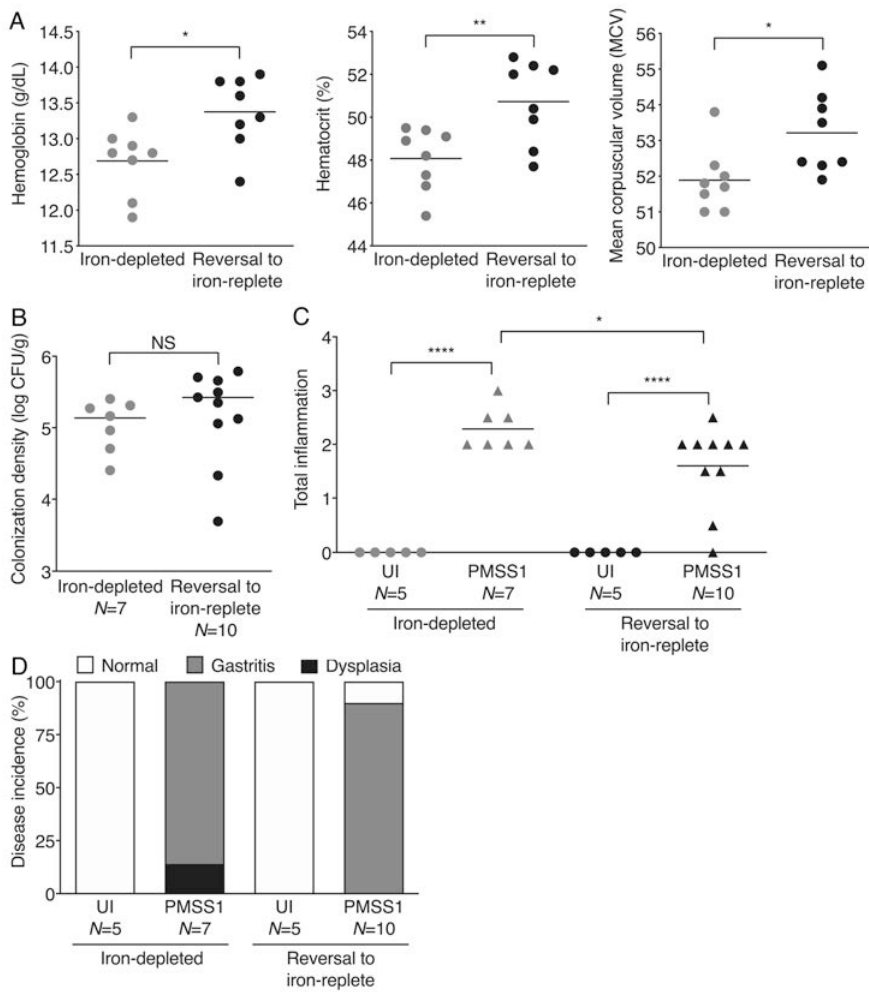
Figure 3. *H. pylori*-induced inflammation and injury under conditions of iron deficiency is reversible. Two groups of male transgenic hypergastrinemic INS-GAS mice were maintained on iron-depleted diets and then challenged with Brucella broth (UI) or *H. pylori* strain PMSS1. Two weeks post-challenge one group was continued on an iron-depleted diet (*N*=12) and the other group was switched to an iron-replete diet (*N*=15). Mice were euthanized eight weeks post-challenge. (**A**) Blood was harvested for CBC analysis from a subset of mice. Hemoglobin, hematocrit, and mean corpuscular volume were assessed as parameters of iron deficiency. (**B**) Gastric tissue was homogenized and plated for quantitative culture. Colonization density is expressed as log colony-forming units/gram of tissue. (**C**) Gastric tissue was fixed, paraffin-embedded, and stained with hematoxylin and eosin. Levels of total gastric inflammation (0-12) were assessed. (**D**) Gastric tissue was also scored for disease incidence. Disease incidence includes normal histopathology, gastritis, and gastric dysplasia. Dysplasia was graded as indefinite dysplasia, low-grade dysplasia, or high-grade dysplasia. Each point represents

data from an individual animal from two independent experiments. Mean values are shown in scatter dot plots. Unpaired parametric t (**A-B**), one-way ordinary ANOVA with Sidak's multiple comparisons (**C**), and Fisher's exact (**D**) tests were used to determine statistical significance. ****, $P<0.0001$; **, $P<0.01$; *, $P<0.05$; NS, not statistically significant.
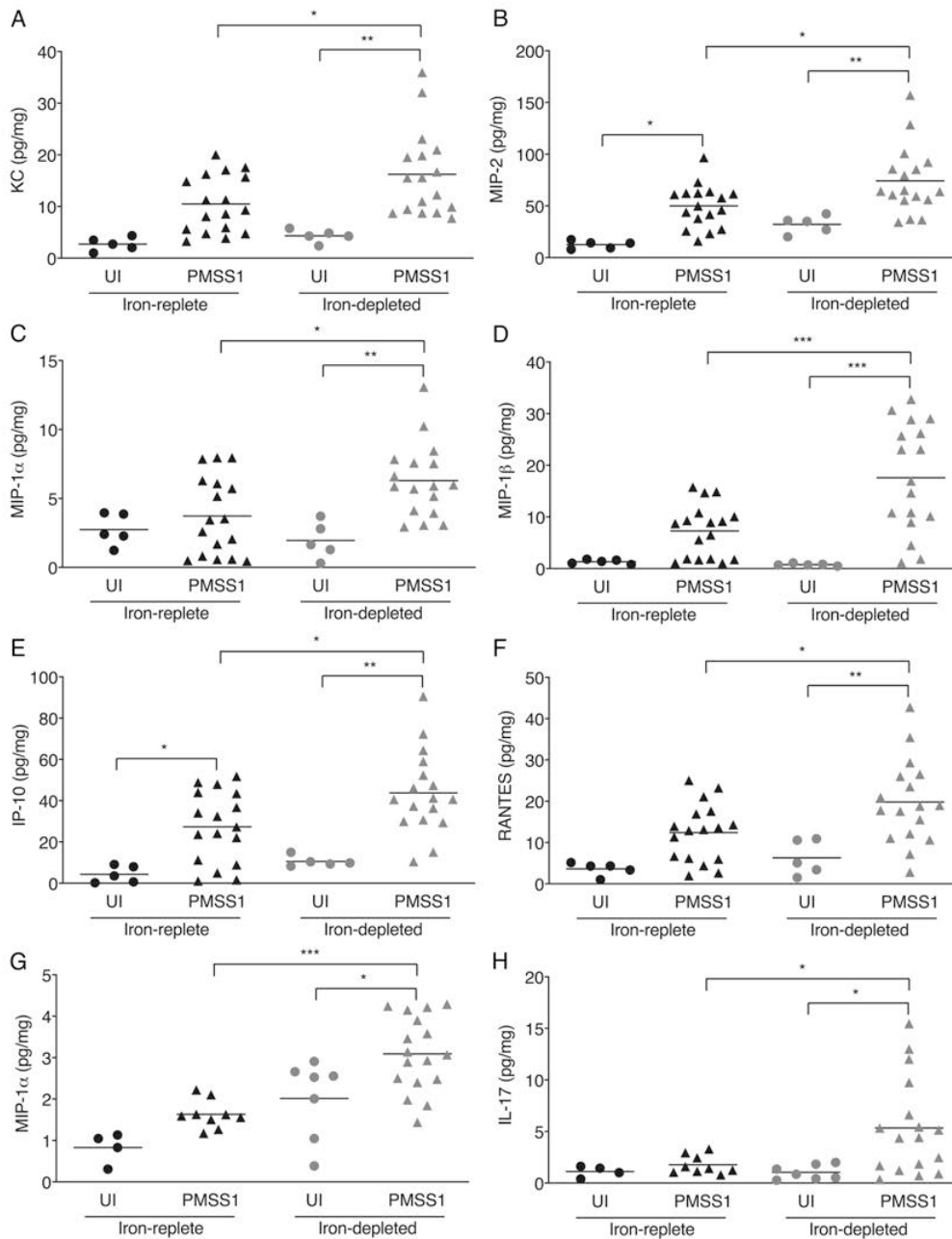
Figure 4. *H. pylori* induces proinflammatory responses in C57BL/6 and INS-GAS mice within the context of iron deficiency. Male and female C57BL/6 and male INS-GAS mice were maintained on iron-replete or iron-depleted diets and then challenged with Brucella broth (UI) or *H. pylori* strain PMSS1. Mice were euthanized eight weeks post-challenge. Gastric tissue was analyzed using a cytokine/chemokine multiplex bead array. Data were acquired and analyzed using the Millipore software platform and expressed as pg of chemokine per mg of gastric tissue. Levels of KC (**A**), MIP-2 (**B**), MIP-1α (**C**), MIP-1β (**D**), IP-10 (**E**), and RANTES (**F**) were

significantly increased by *H. pylori* infection in C57BL/6 mice under conditions of iron deficiency compared to infected mice maintained on iron-replete diets. Levels of MIP-1α (**G**) and IL-17 (**H**) were significantly increased in *H. pylori*-infected INS-GAS mice under conditions of iron deficiency compared to infected mice maintained on iron-replete diets. Each point represents data from an individual animal from three independent experiments. C57BL/6 mice: iron-replete UI (*N*=5) and PMSS1 (*N*=17), iron-depleted UI (*N*=5) and PMSS1 (*N*=17). INS-GAS mice: iron-replete UI (*N*=4) and PMSS1 (*N*=9), iron-depleted UI (*N*=7) and PMSS1 (*N*=17). Mean values are shown in scatter dot plots. One-way ordinary ANOVA with Sidak's multiple comparison test was used to determine statistical significance. Only statistically significant comparisons are denoted. ***, $P<0.001$; **, $P<0.01$; *, $P<0.05$
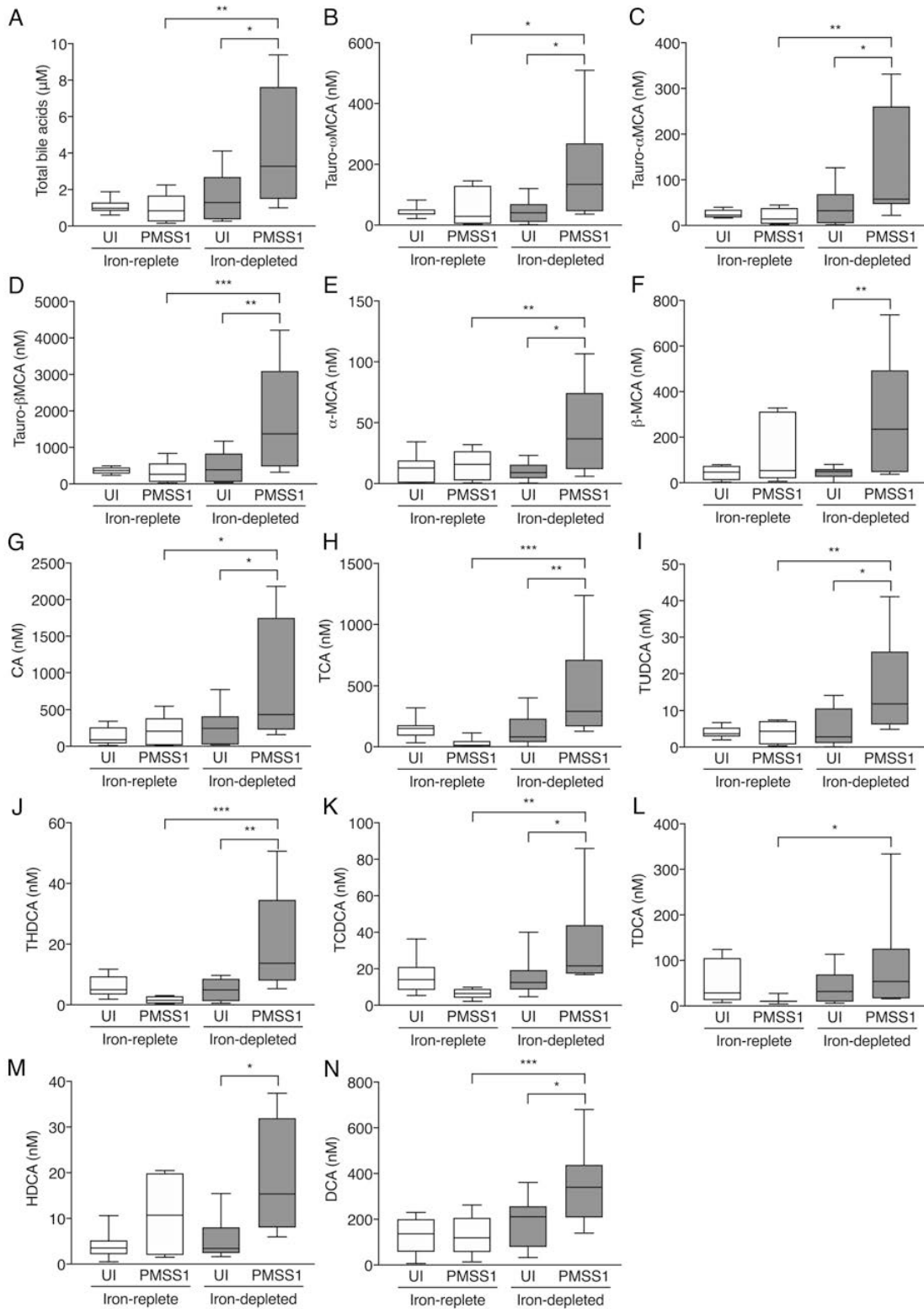
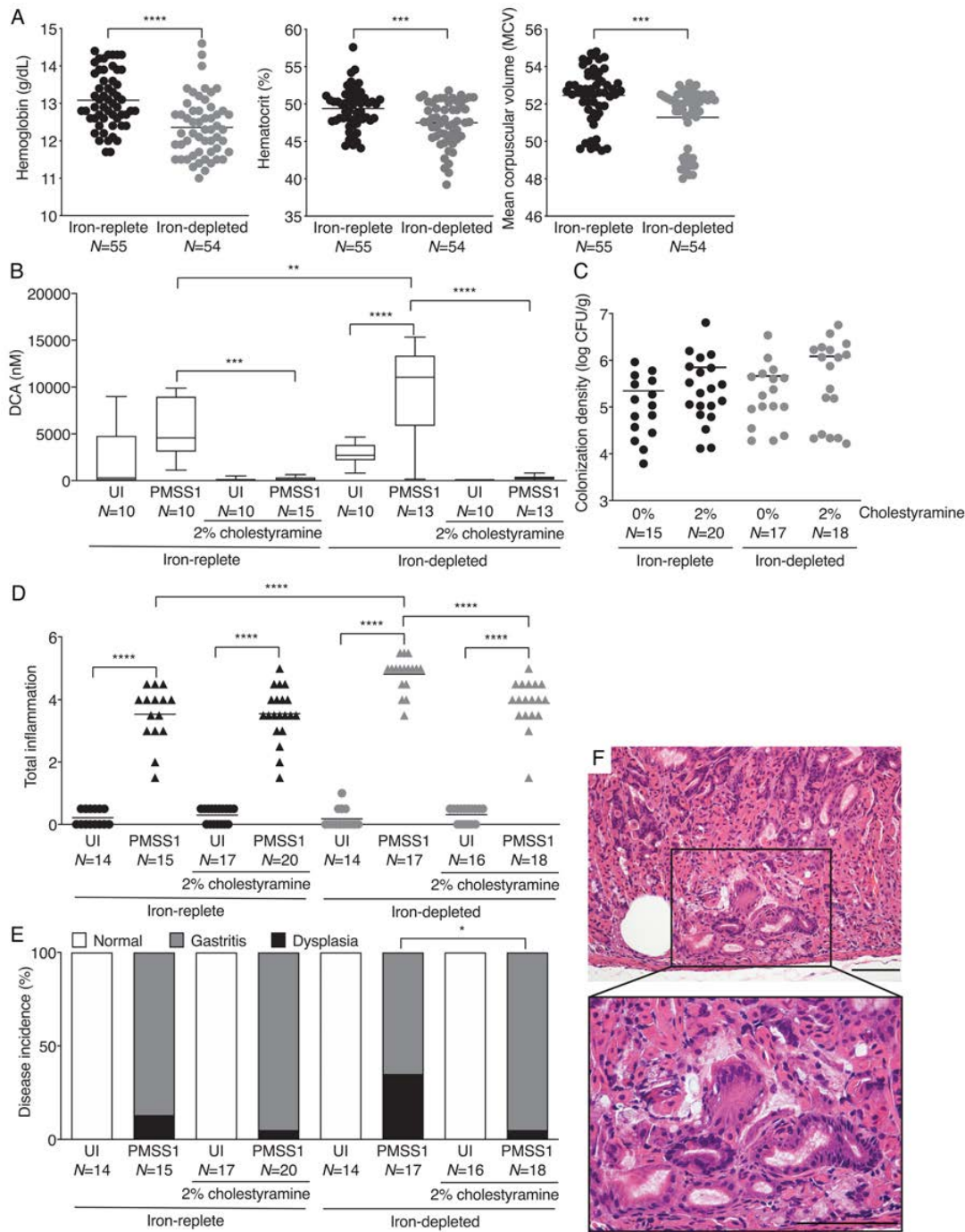**Figure 5. *H. pylori* significantly alters bile acid levels under conditions of iron deficiency in INS-GAS mice.**

Male INS-GAS mice were maintained on iron-replete or iron-depleted diets and then challenged with Brucella

broth (UI) or wild-type *H. pylori* strain PMSS1. Mice were euthanized eight weeks post-challenge. Gastric tissue was processed for targeted bile acid analyses. Total bile acids (**A**) muricholic acids (**B-F**), cholic acids (**G-H**), and deoxycholic acids (**I-N**) were significantly increased by *H. pylori* under conditions of iron deficiency compared to infected mice under iron-replete conditions. Ten mice were analyzed per group from two independent experiments. Median values are shown in box-and-whisker plots with whiskers designating minimum and maximum values. One-way ordinary ANOVA with Sidak's multiple comparison test was used to determine statistical significance. Only statistically significant comparisons are denoted. ***, $P<0.001$; **, $P<0.01$; *, $P<0.05$
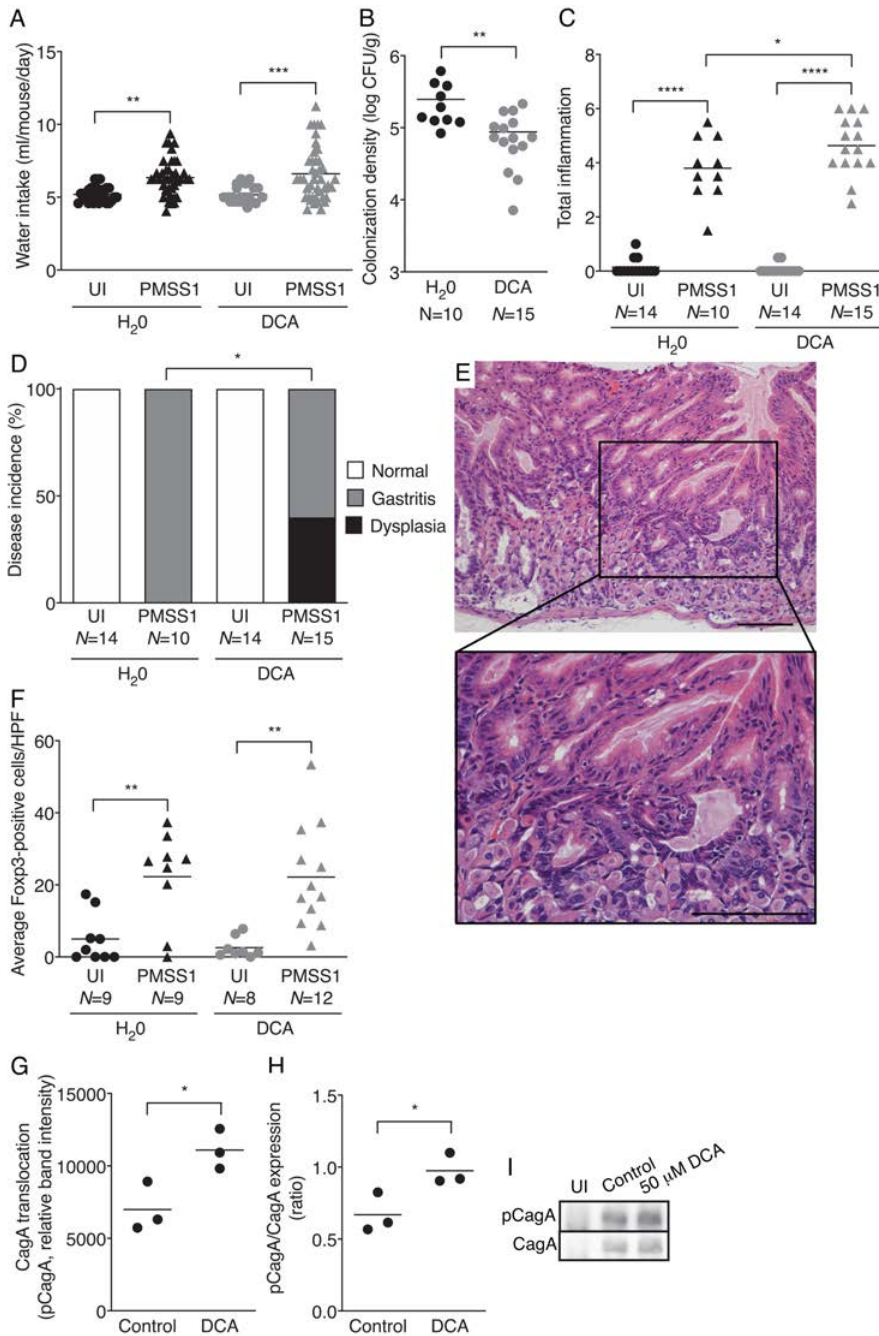
Figure 6. Deoxycholic acid treatment significantly augments *H. pylori*-induced gastric inflammation and injury. Male INS-GAS mice were maintained on an iron-replete standard diet and then challenged with Brucella broth (UI, *N*=28) or *H. pylori* strain PMSS1 (*N*=25). Two weeks following infection, mice received water alone (H₂0) or water supplemented with 100 μM deoxycholic acid (DCA) throughout the course of the experiment. Mice were euthanized six weeks post-challenge. (**A**) Average water consumption was measured. (**B**) Gastric tissue was harvested for quantitative culture. Colonization density is expressed as log colony-forming units/gram of

tissue. Gastric tissue was assessed indices of gastric inflammation (**C**) and disease incidence (**D**). Disease incidence includes normal histopathology, gastritis, and gastric dysplasia. Dysplasia was graded as indefinite dysplasia, low-grade dysplasia, or high-grade dysplasia. (**E**) A representative histologic image of low-grade dysplasia is shown (200X and 400X). Scale bars represent 100 microns. (**F**) The average number of Foxp3-positive cells was assessed by IHC from five high-powered fields (400X). Each point represents data from an individual animal from three independent experiments. (**G-I**) Gastric epithelial cells were co-cultured with *H. pylori* strain PMSS1 and were treated with either vehicle control or 50 μM DCA for six hours and protein lysates were harvested for Western blot analysis. Levels of phosphorylated CagA (**G**) and the ratio of phosphorylated CagA to total CagA was determined (**H**). Representative Western blots are shown (**I**). Mean values are shown in scatter dot plots. Unpaired parametric t (**B**, **G**-**H**), one-way ordinary ANOVA with Sidak's multiple comparisons (**A**, **C**, **F**), and Fisher's exact (**D**) tests were used to determine statistical significance. Only statistically significant comparisons are denoted. ****, $P<0.0001$; ***, $P<0.001$; **, $P<0.01$; *, $P<0.05$

Figure 7. Cholestyramine treatment significantly reduces *H. pylori*-induced inflammation and injury under conditions of iron deficiency in INS-GAS mice. Male INS-GAS mice were maintained on iron-replete (*N*=66) or iron-depleted (*N*=65) diets supplemented with or without 2% cholestyramine (w/w) and then challenged with Brucella broth (UI) or *H. pylori* strain PMSS1. Mice were euthanized eight weeks post-challenge. Whole blood was collected for CBC analysis from a subset of *H. pylori*-infected mice maintained on iron-replete or iron-

depleted diets with or without cholestyramine. (**A**) Hemoglobin, hematocrit, and mean corpuscular volume were assessed as parameters of iron deficiency. (**B**) Gastric tissue was processed for targeted bile acid analyses to assess levels of deoxycholic acid (DCA). (**C**) Gastric tissue was harvested for quantitative culture. Colonization density is expressed as log colony-forming units/gram of tissue. (**D-F**) Gastric tissue was assessed for indices of inflammation (**D**) and disease incidence (**E**). Disease incidence includes normal histopathology, gastritis, and gastric dysplasia. Dysplasia was graded as indefinite dysplasia (borderline nuclear and architectural epithelial changes that do not completely fit the patterns of dysplasia), low-grade or high-grade dysplasia. (**F**) A representative histologic image of indefinite dysplasia is shown (200X and 400X). Scale bars represent 100 microns. Each point represents data from an individual animal from three independent experiments. Mean values are shown in scatter dot plots. Median values are shown in box-and-whisker plots with whiskers designating minimum and maximum values. Unpaired parametric t (**A**), one-way ordinary ANOVA with Sidak's multiple comparisons (**B-D**), and Fisher's exact (**E**) tests were used to determine statistical significance. Only statistically significant comparisons are denoted. ****, $P<0.0001$; ***, $P<0.005$; **, $P<0.01$; *, $P<0.05$
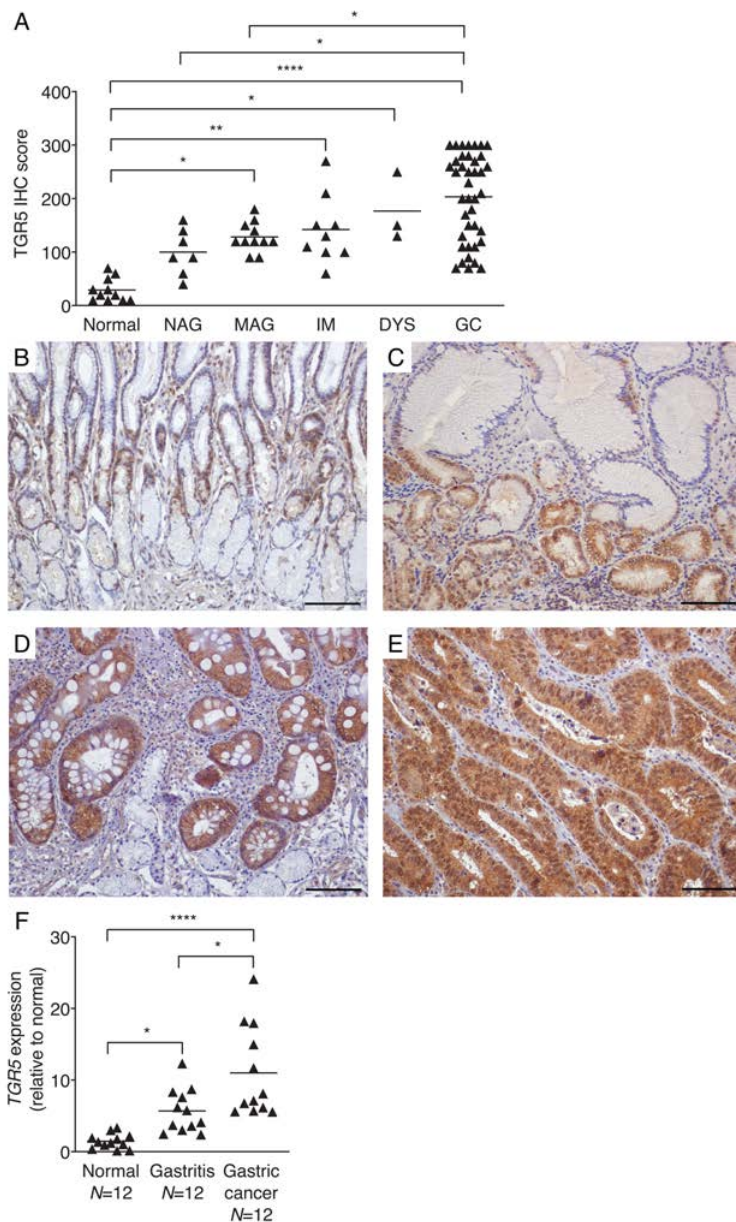
Figure 8. TGR5 expression parallels the severity of gastric disease. (**A**) TGR5 protein expression was evaluated by immunohistochemistry (IHC) in human gastric tissues from a gastric cancer tissue microarray (TMA). A single pathologist assessed the percentage of TGR5-positive cells and the intensity of TGR5 staining. The IHC score reflects the percentage of cells positive for TGR5, multiplied by the intensity of staining, as previously described (61). TGR5 staining was assessed in gastric tissue sections from patients with no pathology (normal, *N*=11), non-atrophic gastritis (NAG, *N*=7), multifocal atrophic gastritis (MAG; *N*=11) without intestinal metaplasia, intestinal metaplasia (IM, *N*=9), dysplasia (DYS, *N*=3), and gastric cancer (GC, *N*=40). (**B-E**)

Representative images of TGR5 protein expression in normal gastric tissue sections (**B**), or gastric tissue sections with multifocal atrophic gastritis (**C**), intestinal metaplasia (**D**), and gastric cancer (**E**) are shown (200X). Scale bars represent 100 microns. (**F**) RNA was extracted from normal gastric tissue (*N*=12), gastric tissues with gastritis alone (*N*=12), and gastric tissues with gastric adenocarcinoma (*N*=12). *TGR5* mRNA expression levels were standardized to levels of *GAPDH* mRNA expression and are shown as fold relative to normal (2^-($\Delta\Delta$CT)). Mean values are shown in scatter dot plots. One-way ordinary ANOVA with Sidak's multiple comparison test was used to determine statistical significance. Only statistically significant comparisons are denoted. ****, *P*<0.0001; **, *P*<0.01; *, *P*<0.05

Table 1. Demographic and clinical characteristics of human cohort (*N*=416,885)

Variable	Exposed *N*=19,634	Non-exposed *N*=397,251	*P* value[c]
Age, mean ± SD[A]	57 ± 14	54 ± 16	*P*<0.001
Male sex, % (*N*[B])	88% (17,285)	89% (351,819)	*P*=0.02
Race/Ethnicity, % (*N*[B]) White, non-Hispanic	70% (13,679)	63% (248,369)	*P*<0.001
Current/former smoker, % (*N*[B])	44% (8,593)	37% (148,697)	*P*<0.001
H. pylori positive, % (*N*[B])	32% (6,345)	34% (136,200)	*P*<0.001

[A]SD=standard deviation

[B]*N*=number

[c]Wilcoxon test was used to determine statistical significance for age (continuous variable), and the Pearson's Chi-squared test was used for all other categorical variables.

Table 2. Factors associated with incident gastric cancer based on multivariable Cox regression analysis

Variable	Hazard ratio (95% CI)	*P* value
Age[A]	4.17 (3.62-4.79)	*P*<0.001
Male sex (reference: female)	2.15 (1.67-2.78)	*P*<0.001
Race/Ethnicity (reference: white, non-Hispanic)	1.46 (1.33-1.60)	*P*<0.001
Current/former smoker (reference: nonsmoker)	1.34 (1.23-1.47)	*P*<0.001
H. pylori positive (reference: *H. pylori* negative)	1.47 (1.34-1.61)	*P*<0.001
Bile acid-sequestrant use 1% total days[B] (reference: no use)	0.92 (0.86-0.98)	*P*<0.01
Bile acid-sequestrant use 5% total days[B] (reference: no use)	0.70 (0.53-0.92)	*P*=0.015
Bile acid-sequestrant use 20% total days[B] (reference: no use)	0.71 (0.48-1.04)	*P*=0.073

[A]The age covariate was fit via a nonlinear spline. The HR (95%) presented represents the comparison of the 77th versus 25th percentile (reference) of age for the cohort. This corresponds to age 65 versus 43 years old.

[B]The proportion of total days exposed to bile acid-sequestrants was fit via a nonlinear spline. Effect sizes were evaluated at three different exposure thresholds, 1%, 5%, and 20% of days, and all relative to no use/exposure (reference). These thresholds correspond to the 22nd, 67th, and 91st percentiles, respectively, among individuals with any use of bile acid-sequestrant medications.

Table 3. Demographic and clinical characteristics of human gastric samples

Variable	Normal N=12	Gastritis N=12	Gastric adenocarcinoma N=12
Age, mean ± SD	64 ± 10	69 ± 6	65 ± 11
Male sex, %	50%	83%	67%
Race/Ethnicity, % White, non-Hispanic	83%	67%	100%